Local4Global

SYSTEM-OF-SYSTEMS THAT ACT LOCALLY FOR OPTIMIZING GLOBALLY

611538, FP7-ICT-2013.3.4

Deliverable D4.1.1

TSoS Distributed Optimization (2nd version)

Deliverable Version:	D4.1.1, v.2.1
Document Identifier:	local4global_wp4_d4.1.1_ETH_v2.1.pdf
Preparation Date:	August 15, 2015
Document Status:	Final
Author(s):	Paul Beuchat, Angelos Georghiou, Xiaojing Zhang, Georgios Darivianakis, Roy R. Smith, John Lygeros and the Local4Global consortium
Dissemination Level:	PU - Public

Project funded by the European Community in the 7th Framework Programme

EU FP7 - SMALL/MEDIUM-SCALE FOCUSED RESEARCH PROJECT (STREP), FP7-ICT-2013.3.4: ADVANCED COMPUTING, EMBEDDED AND CONTROL SYSTEMS

D) FROM ANALYZING TO CONTROLLING BEHAVIOUR OF SYSTEM OF SYSTEMS (SOS)

SEVENTH FRAMEWORK PROGRAMME

European Commission
Information Society and Media

Deliverable SUMMARY SHEET

Deliverable Details	
Type of Document:	Deliverable
Document Reference #:	D4.1.1
Title:	TSoS Distributed Optimization (2nd version)
Version Number:	2.1
Preparation Date:	August 15, 2015
Delivery Date:	August 15, 2015
Author(s):	Paul Beuchat, Angelos Georghiou, Xiaojing Zhang, Georgios Darivianakis, Roy R. Smith, John Lygeros and the Local4Global consortium
Document Identifier:	local4global_wp4_d4.1.1_ETH_v2.1.pdf
Document Status:	Final
Dissemination Level:	PU - Public

Project Details	
Project Acronym:	Local4Global
Project Title:	SYSTEM-OF-SYSTEMS THAT ACT LOCALLY FOR OPTIMIZING GLOBALLY
Project Number:	611538
Call Identifier:	FP7-ICT-2013.3.4
Call Theme:	ADVANCED COMPUTING, EMBEDDED AND CONTROL SYSTEMS
Project Coordinator:	CERTH – Centre for Research and Technology – Hellas
Participating Partners:	CERTH – Centre for Research and Technology – Hellas; ETHZ – Eidgenössische Technische Hochschule Zürich; RWTH – RWTH Aachen University; IK4 – IK4 TEKNIKER; TRV – TRANSVER GmbH; TUC – Technical University of Crete; TUM – Technische Universtität Muenchen;
Instrument:	STREP
Contract Start Date:	October 1, 2013
Duration:	36 Months

Deliverable D4.1.1: Short Description
This document presents the theorical tools which are going to be used in the L4G project. The aim of this deliverable is to develop optimization based techniques that will be later used to address the two case-studies. All the theory presented are in line with the work carried out by the consortium partners in the Centre for Research and Technology and the Technical University of Crete.
Keywords: TSoS, L4G platform, optimization problems, dynamic programming, decision making under uncertainty, decision rules, distributed optimization algorithms

Deliverable D4.1.1: Revision History			
Version:	**Date:**	**Status:**	**Comments**
0.1	**01/12/2014**	**Draft**	**Initial draft, Building energy management section**
0.2	**01/02/2015**	**Draft**	**Second draft (Munich meeting), Randomised MPC**
0.3	**10/04/2015**	**Draft**	**Completed draft**
0.4	**20/04/2015**	**Draft**	**Internal review**
1.0	**05/05/2015**	**Submitted**	**ETHZ final vesion**
2.0	**28/07/2015**	**Draft**	**Internal review**
2.1	**15/08/2015**	**Final**	**Final version, revised based on Reviewer and Commission comments.**

Table Of Contents

Executive Summary

Technical System of Systems (TSoS) is a term used to characterise the structure of the underlying system. In this setting, a collection of individual systems are pooled together, sharing resources and capabilities, to create a new more complex entity offering greater functionality and performance than individual constituent systems. Continuing the work presented in Deliverable 3.3, this deliverable presents formulation of such Technical System of Systems is the context of building control, which is one of the case studies of L4G, and develops solution techniques for addressing worst-case, decision making methods, in a robust and randomized manner. The solution methods presented allow to address generic Technical System of Systems in both a centralised and decentralised/distributed manner. The deliverable is split into two main sections, and addresses (*i*) robust and (*ii*) stochastic optimization problems.

In the first part of the deliverable, we utilize the solution techniques know as the *decision rule approximation*, a solution technique which was partly developed and presented in Section 4 of Deliverable 3.3, to formulate and solve a building control problem. Building energy management is an active field or research since the potential in energy savings can be substantial. Nevertheless, the opportunities for large saving of individual buildings can be limited by the flexibility of the installed climate control devices and the individual construction characteristics. We use the energy hub concept which allows one to manage a collection of buildings in a cooperative manner, by providing opportunities for load shifting between buildings and the sharing of expensive but energy efficient equipment housed in the hub, such as heat pumps, boilers, batteries. This problem can be formulated as a robust optimization and we demonstrate that the proposed decision rule approximation can provide significant benefits compared to traditional solution techniques.

In the second part of the deliverable, we combine ideas from robust and randomized optimization, and propose a novel approximation for addressing chance-constrainted, multistage optimization problems. This type of problem structures are very common in Stochastic Model Predictive Control problems for constrained linear systems subject to additive disturbance. We show that the proposed approximation can greatly reduce conservatism of

the solution while exhibiting favorable scaling properties with respect to the prediction horizon. The approximation is presented from a centralized optimization point of view, but our results can readily be extend to distributed problems using the solution method proposed and presented in Section 5 of Deliverable 3.3, which is based on the alternating direction method of multipliers, (ADMM algorithm).

1 Introduction

1.1 Description of Task 4.1.1

In this task, we will investigate the potential of two classes of methods to address TSoS distributed, real-time optimization problems in the Local4Global context.

- Worst-case, real-time decision making methods. Real-time decision making methods for generating decisions in a worst-case or robust manner. Such methods are applicable in cases where it is essential to provide firm guarantees about the behaviour of a system, e.g., that some safety-critical threshold will not be exceeded under any circumstances. Recent efforts in distributed optimization (such as the alternating direction method of multipliers) have provided hope that, at least for convex optimization problems such robust methods can also be deployed in a distributed fashion. The numerical methods developed will be based on a detailed understanding and exploitation of the internal structure in the model of the system to be controlled.
- Randomized, real-time decision making methods. For those cases in which the models developed have very little exploitable internal structure, an approach entirely different will be required. For such cases, this task will develop real-time decision making methods based on randomized real-time decision making. We will investigate a range of methods, from simple Monte-Carlo methods to randomly select decision variables to more sophisticated Markov Chain Monte-Carlo real-time decision making and simulated annealing methods, which explore the decision space in a systematic (albeit random) way. We will investigate approaches to deploy these methods in a distributed manner by exploiting advances in distributed randomized algorithms such as interacting particle systems and MCMC-within-particle systems. In each case, actions are selected from the space of possible decisions and then evaluated by treating the models as a (possibly stochastic) "oracle" of the system response to decisions.

1.2 Description of Deliverable 4.1.1

The deliverable is split into two main sections to address (*i*) Worst-case, real-time decision making methods and (*ii*) randomized, real-time decision making methods. In Section 2, we present formulations and solution methods for a multistage stochastic optimization programs in the context of building control which is one of the case studies for L4G. Section 2 can be summarised as follows:

- Building energy management is an active field or research since the potential in energy savings can be substantial. Nevertheless, the opportunities for large saving of individual buildings can be limited by the flexibility of the installed climate control devices and the individual construction characteristics. The energy hub concept allows one to manage a collection of buildings in a cooperative manner, by providing opportunities for load shifting between buildings and the sharing of expensive but energy efficient equipment housed in the hub, such as heat pumps, boilers, batteries. Typically, control design for the buildings and the energy hub are done separately, underutilizing the potential flexibility provided by the interconnected system. To address these issues, we propose a unified framework for controlling the operation of the energy hub and the buildings it connects to. By modeling all exogenous disturbance parameters as stochastic processes, and by using state-space representation of the building dynamics, we formulate a multistage stochastic optimization problem to minimize the total energy consumption of the system in a cooperative manner. We solve the resulting infinite dimensional optimization problem using a decision rule approximation, and we benchmark its performance on a numerical study, comparing it with established solution techniques.

In Section 3, we develop randomized solution algorithms for the solution of multistage stochastic optimization programs that involve chance constraints. These types of problems typically arise in the context of building control. Section 3 can be summarised as follows:

- We consider Stochastic Model Predictive Control problems for constrained linear systems subject to additive disturbance. A popular method for solving the associated chance constrained optimization problem is by means of randomization, in which the chance constraints are replaced by a finite number of sampled constraints, each corresponding to a disturbance realization. Earlier approaches in this direction lead to computationally expensive problems, whose solutions are typically very conservative both in terms of cost and violation probabilities. A way of overcoming this conservatism, is to use piecewise affine (PWA) policies, which offer more flexibility than conventional open-loop and affine policies. Unfortunately, the straight-forward application of randomized methods towards PWA policies will lead to computationally demanding problems, that can only be solved for problems of small sizes. To address this issue, we propose an alternative method based on a combination of randomized and robust optimization. We show that the resulting approximation can greatly reduce conservatism of the solution while exhibiting favorable scaling properties with respect to the prediction horizon. The efficacy of the proposed approach relative to standard techniques is demonstrated in an inventory control problem.

This work presented in deliverable 4.1.1 will be extended in deliverable 4.1.2 in the following ways: The current theory supports only linear systems. To address this, we are developing solution methods in the context of approximate dynamic programming that will allow to (i) consider systems with polynomial structure in the dynamics, and (ii) it will allow for the distributed and decentralised control designs. This will enable to push the operational envelop of these solution methods for addressing complex systems, such as non-linear systems arising in building control problems where the dynamics of each constituent component is modelled in greater detail.

1.3 Connection to the L4G use cases

The theoretical contributions presented in this deliverable have been developed to be well suited for the L4G use cases, and specifically tailored to address the challenges associated with the building TSoS use case. In particular,

- In the first part of the deliverable, we leverage prior work (BRCM toolbox [50]) to develop state space representation of the buildings energy management system, and proposed the use of modern robust optimization techniques known as decision rules, for approximating the resulting multistage stochastic optimization problem. We compared our results to traditional deterministic and robust optimization techniques, assessing their potential benefits prior to the real implemented on the building TSoS use case. Although presented for an energy hub, the control approach presented is flexible and can be readily adapted to consider one building as the entire TSoS. In a single building setting, each room (or collection of rooms) is considered a sub-system and the shared resources are the climate control equipment installed in the basement, such as heat pumps, boilers, batteries. We would like to note that the solution methods discussed in the first part of the deliverable, are presented from a centralized optimization point of view. Nevertheless, all solution algorithms were developed having in mind a decentralised implementation scheme. Indeed, our results can be directly extend to distributed problems using the solution method proposed and presented in Section 5 of Deliverable 3.3, which is based on the alternating direction method of multipliers, (ADMM algorithm). Combining the theoretical contributions in the two documents results to a ready to use method for the actual implementation of the building use case. In collaboration with the project partners from RWTH Aachen University, we are currently testing the performance of the proposed methods in a simulated environment, prior to the actual implementation on the real system.

- In the second part of the deliverable, we address a crucial issue associated with the modelling of the uncertainty when dealing with stochastic dynamical models. This issue is particularly relevant in the building TSoS use case where the uncertainty associated with the exogenous disturbances of temperature, solar radiation and internal gains of the buildings, are the parameters driving the heat dynamics of a building. The solution method developed is data-driven and does not require any model structure on the evolution of the exogenous disturbances. This feature makes it particularly useful in a real world application where the dynamical model governing the evolution of the uncertain parameters is hard to be described analytically and can change significantly over time. Furthermore, the solution method developed is compatible with the first part of the deliverable and can be directly applied in the building use case. In particular, the methodology is based on the decision rule approximation, and uses robust optimization techniques to handle the stochastic chance constraints program. Due to this compatibility, one can directly use the decentralised implementation scheme proposed and presented in Section 5 of Deliverable 3.3, without any further refinement in the method.

We end this section by emphasizing that the solution method for discrete optimization problems under uncertainty presented in Deliverable 3.3 (Section 4), is a natural extension in both the first and second parts of the current deliverable, and can be used directly for both the building and traffic TSoS use case. Indeed, since the methodology allows to optimize over both discrete and continuous decisions, one can model with high fidelity discrete decisions in the building such as on-off processes, as well as, discrete traffic lights control in the traffic use case.

2 A Stochastic Optimization Approach to Cooperative Building Energy Management via an Energy Hub

Recent studies [29, 36] have shown that around three quarters of the total electricity consumption in Europe and the US is attributed to buildings, with almost half of the energy being used for the building's climate control. In addition, European standards require office buildings to maintain their room temperature within given ranges (typically 21°C to 25°C) during working hours, with only minor violations during the course of a year [15]. Therefore, substantial efforts has been devoted for the optimal control of climate control devices to reduce their impact on electricity consumption [33, 38, 57, 61]. Unfortunately, experimental verifications have shown that these savings are limited by the flexibility of the devices and the construction characteristics of individual building [47, 2, 5, 48].

To reach further savings, economies of scales need to be exploited. This can be achieved in two ways: (*i*) Office buildings aggregation provides the opportunity to manage collectively their energy needs, taking advantage of the intraday price fluctuations in the electricity price and performing efficient load shifting between buildings; (*ii*) Sharing the use of energy efficient equipment such as heat pumps, boilers, batteries, as well photovoltics, which are usually prohibitively expensive to be purchased and operated by a single building unit. The concept of the *energy hub* serves this dual purpose by housing the expensive components shared between buildings and provides the interface between the building community and the energy grid [19, 20].

The energy hub idea is a rather recent concept, with the main body of the literature separating the optimal control of the energy hub and the buildings connected to the system. Indeed, a number of papers treats the building energy demands as exogenous signals, which are typically estimated using building simulation environments such as the EnergyPlus [14]. These models include both deterministic [16, 17] and stochastic [41] formulations, and aim to optimally control the devices within the energy hub. More complex systems with multiple energy hubs also appear in the literature, where deterministic model predictive control approaches are used for the optimal operation of the system [1]. The downside of decoupling the operation of the energy hub and the interconnected buildings, is the underutilization of the load shifting capabilities of the buildings in the interconnected system and the suboptimal operation of the devices present in the energy hub.

The goal of this is section is to present a unified framework for controlling the operation of the energy hub and the buildings it connects. The proposed methodology minimizes the total energy consumption of the building community in a cooperative fashion. To this end, we consider the stochastic state-space representation for the building dynamics proposed in [50] and formulate a stochastic state-space models for the devices present in the energy hub base on the work of [16, 18, 56]. We use modern robust optimization techniques known as *decision rules*, [4, 23] for approximating the resulting multistage stochastic optimization problem, and we compare our results to traditional deterministic and robust optimization techniques.

The section is organised as follows. In Section 2.1 we present the model description for the underline system, and in Section 2.2 we formulate the resulting optimization problem. The decision rules solution method is summarized in Section 2.3 and in Section 2.4 we present our computational results.

Notation: All random vectors appearing in this section are defined on an abstract probability space $(\Omega, \mathcal{F}, \mathbb{P})$, where $\mathbb{E}(\cdot)$ denotes the expectation operator with respect to $\mathbb{P}$. Random vectors are represented in boldface, while their realisations are represented by the same symbols in normal face. For any random vector $\boldsymbol{\xi}$, we let $\sigma(\boldsymbol{\xi})$ be the σ-algebra of $\mathcal{F}$ generated by $\boldsymbol{\xi}$, while $\mathcal{L}^2(\boldsymbol{\xi}) = \mathcal{L}^2(\Omega, \sigma(\boldsymbol{\xi}), \mathbb{P})$ denotes the space of all $\sigma(\boldsymbol{\xi})$-measurable square-integrable random variables. This technical assumption ensures that the expectation remains bounded. *All equalities and inequalities involving random variables are assumed to hold with probability 1.* Finally, $\boldsymbol{e}$ denotes the vector whose components are all ones and its size will be clear from the context.

2.1 Model description

In this section, we use the illustrative example depicted in Fig. 1 to descibe the governing dynamics of the underline system. The system can be described by a discrete time, bi-linear model, in which the dynamics are affected by stochastic exogenous disturbances.

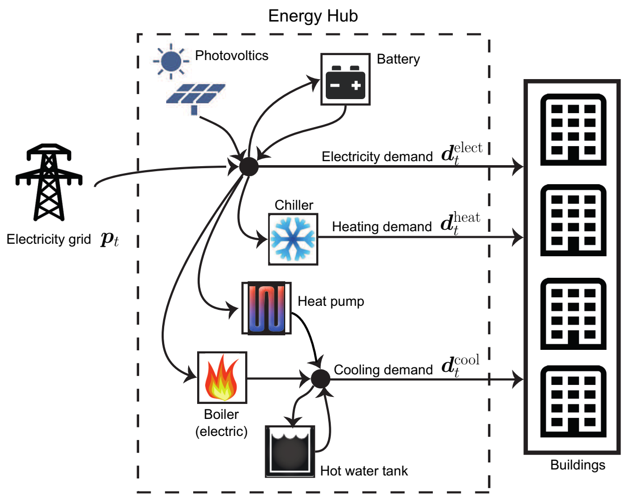

Figure 1: *District electricity, heating and cooling network.*

We assume that these disturbances evolve according to given stochastic processes $\{\boldsymbol{\xi}_t\}_{t\in\mathcal{T}}$, where $\mathcal{T} = \{1, \ldots, T\}$, and T is the length of the horizon considered with an hourly time discretization. Here, vector $\boldsymbol{\xi}_t$ encompasses all stochastic processes that appear in the problem, including the stochastic evolution of the temperature, solar radiation and internal gains of the buildings. We also denote by $\boldsymbol{I}_t$ the information basis for the operating decisions taken at stage t. The structure of $\boldsymbol{I}_t$ will dictate the behaviour of the corresponding operating decisions; in principle it can contain any information that is relevant to devices at decision time t. This can include the full or a partial history of the stochastic processes $\boldsymbol{\xi}_t$ as well as forecasts of some future states of the stochastic processes. Note that all quantities appearing in the chapter are real numbers, with the size of the corresponding vectors will be clear from the context.

2.1.1 Structure of the system

The system comprises a set of buildings, denoted by $\mathcal{B}$, and an energy hub. The buildings meet all their energy requirements from the energy hub. The energy hub serves two purposes: (i) It houses the expensive components shared by the buildings, including energy conversion units, such as heat pump, chiller, boiler, photovoltaics, as well as storage units, such as batteries and hot water tanks; (ii) It acts as an energy balancing node, by providing the interface between the energy grid, and the buildings connected to it. At time t, each building $i \in \mathcal{B}$ can have three energy demand requirements: (i) demand for electricity $\boldsymbol{d}_{t,i}^{\text{elect}} \in \mathcal{L}^2(\boldsymbol{I}_t)$, (*ii*) demand for heating $\boldsymbol{d}_{t,i}^{\text{heat}} \in \mathcal{L}^2(\boldsymbol{I}_t)$, and (*iii*) demand for cooling $\boldsymbol{d}_{t,i}^{\text{cool}} \in \mathcal{L}^2(\boldsymbol{I}_t)$. Note that $\{\boldsymbol{d}_{t,i}^{\text{elect}}\}_{t\in\mathcal{T}}$, $\{\boldsymbol{d}_{t,i}^{\text{heat}}\}_{t\in\mathcal{T}}$, $\{\boldsymbol{d}_{t,i}^{\text{cool}}\}_{t\in\mathcal{T}}$ are in fact stochastic processes which are affected by exogenous stochastic process $\{\boldsymbol{\xi}_t\}_{t\in\mathcal{T}}$. We denote the energy purchased by the energy hub from the grid at time t by $\boldsymbol{p}_t \in \mathcal{L}^2(\boldsymbol{I}_t)$.

2.1.2 Energy hub dynamics

In the following, we denote by $\mathcal{D}$ the set of devices controlled by the energy hub. The following dynamical system describes the evolution of energy $\boldsymbol{x}_{t,i}$ in a particular device $i \in \mathcal{D}$:

$$\left.\begin{aligned} \boldsymbol{x}_{t+1,i} &= A_i \boldsymbol{x}_{t,i} + B_i \boldsymbol{u}_{t,i} + C_i \boldsymbol{\xi}_t, \\ (\boldsymbol{x}_{t,i}, \boldsymbol{u}_{t,i}^{\text{in}}, \boldsymbol{u}_{t,i}^{\text{out}}, \boldsymbol{\xi}_t) &\in \mathcal{C}_{t,i}, \\ \boldsymbol{u}_{t,i}^{\text{in}}, \boldsymbol{u}_{t,i}^{\text{out}} &\in \mathcal{L}^2(\boldsymbol{I}_t), \end{aligned}\right\} \forall t \in \mathcal{T}. \tag{1}$$

Here, $\boldsymbol{u}_{t,i}^{\text{in}}$ and $\boldsymbol{u}_{t,i}^{\text{out}}$ are the controlled inputs and outputs of energy from the device, respectively. Set $\mathcal{C}_{t,i}$ describes state and input constraints for device i.

The three energy carriers (electrical, heating, cooling) give rise to three energy balancing constraints. The electricity balancing constraint is given by

$$\boldsymbol{p}_t + \sum_{i\in \mathrm{E}_+} \boldsymbol{u}_{t,i}^{\text{out}} = \sum_{i\in \mathrm{E}_-} \boldsymbol{u}_{t,i}^{\text{in}} + \sum_{i\in\mathcal{B}} \boldsymbol{d}_{t,i}^{\text{elect}}, \quad \forall t \in \mathcal{T}, \tag{2a}$$

where $\mathrm{E}_+ \subseteq \mathcal{D}$ and $\mathrm{E}_- \subseteq \mathcal{D}$ are the set of devices that can contribute and consume electricity, respectively, within the energy hub. In the example depicted in Figure 1, $\mathrm{E}_+ = \{\text{photovoltaics, battery}\}$ and $\mathrm{E}_- = \{\text{heat pump, chiller, boiler, battery}\}$. The heating energy balancing constraint is given by

$$\sum_{i\in \mathrm{H}_+} \boldsymbol{u}_{t,i}^{\text{out}} = \sum_{i\in \mathrm{H}_-} \boldsymbol{u}_{t,i}^{\text{in}} + \sum_{i\in\mathcal{B}} \boldsymbol{d}_{t,i}^{\text{heat}}, \quad \forall t \in \mathcal{T}, \tag{2b}$$

where $H_+ \subseteq \mathcal{D}$ and $H_- \subseteq \mathcal{D}$ are the set of devices that can contribute and consume heat energy, respectively, within the energy hub. In Figure 1, these sets are defined as $\mathrm{H}_+ = \{\text{heat pump, boiler, hot water tank}\}$ and $\mathrm{H}_- = \{\text{hot water tank}\}$. Finally, the cooling energy balancing constraint is as follows

$$\sum_{i \in C_+} \boldsymbol{u}_{t,i}^{\text{out}} = \sum_{i \in \mathcal{B}} \boldsymbol{d}_{t,i}^{\text{cool}}, \quad \forall t \in \mathcal{T}, \tag{2c}$$

with $C_+ \subseteq \mathcal{D}$, and $C_+ = \{\text{chiller}\}$ in our running example.

We close this section by defining the following constraint set for the energy hub:

$$\text{EH} := \Big\{ \{\boldsymbol{p}_t\}_{t \in \mathcal{T}}, \{\boldsymbol{d}_t\}_{t \in \mathcal{T}} : \exists \{\boldsymbol{u}_t^{\text{in}}\}_{t \in \mathcal{T}}, \{\boldsymbol{u}_t^{\text{out}}\}_{t \in \mathcal{T}} \text{ such that (1), (2) hold} \Big\}.$$

where $\boldsymbol{d}_t = (\boldsymbol{d}_t^{\text{elect}}, \boldsymbol{d}_t^{\text{heat}}, \boldsymbol{d}_t^{\text{cool}})$, $\boldsymbol{u}_t^{\text{in}} = (\boldsymbol{u}_{t,1}^{\text{in}}, \ldots, \boldsymbol{u}_{t,|\mathcal{D}|}^{\text{in}})$ and $\boldsymbol{u}_t^{\text{out}} = (\boldsymbol{u}_{t,1}^{\text{out}}, \ldots, \boldsymbol{u}_{t,|\mathcal{D}|}^{\text{out}})$.

2.1.3 Building dynamics

We use the building model developed in [50] which gives rise to a bi-linear state-space model. The model captures the evolution of temperature in the building and has as states the temperatures of the individual rooms, walls, floors and ceiling layers of the building, and as control inputs the energy provided by the radiators, blinds position, air handling units (AHU) and thermally activated building structures (TABS). Models of this type can be developed using capacitance-resistance model of the building and their accuracy was benchmarked against established building simulation software such as EnergyPlus [14] and validated against real buildings [49]. For each building $i \in \mathcal{B}$ and time point $t \in \mathcal{T}$, the bi-linear dynamic are given by:

$$\begin{aligned} \boldsymbol{x}_{t+1,i} = A_i \boldsymbol{x}_{t,i} + B_i \boldsymbol{u}_{t,i} + C_i \boldsymbol{\xi}_t & \\ + \sum_{j \in \mathcal{D}_i^{\text{b}}} \left(D_{i,j} \boldsymbol{\xi}_t + E_{i,j} \boldsymbol{x}_{t,i} \right) \boldsymbol{u}_{t,i,j}, & \\ (\boldsymbol{u}_i, \boldsymbol{\xi}) \in \mathcal{U}_i, \; \boldsymbol{u}_{t,i} \in \mathcal{L}^2(\boldsymbol{I}_t), & \end{aligned} \tag{3a}$$

where $\mathcal{D}_i^{\text{b}} = \{\text{radiators, blinds position, AHU, TABS}\}$ is the set of devices present in the building. The units of states $\boldsymbol{x}_{t,i}$ are in degrees Celsius. $\mathcal{U}_i$ is the set of linear coupling constraints between inputs and disturbances. We define $\boldsymbol{x}_{t,i}^{\text{room}}$ to be the subvector of $\boldsymbol{x}_{t,i}$

which denotes the states associated with room temperatures in the building. The following constraints ensure that the temperature in the rooms $\boldsymbol{x}_{t,i}^{\text{room}}$ remain within user comfort ranges:

$$\text{lb}_{t,i} \leq \boldsymbol{x}_{t,i}^{\text{room}} \leq \text{ub}_{t,i}, \quad \forall t \in \mathcal{T}, \tag{3b}$$

where $\text{lb}_{t,i}$ and $\text{ub}_{t,i}$ are lower and upper bounds on the room temperature at time t and building i. We will refer to constraint set (3b) as the *comfort constraints*. We emphasize that these ranges are time varying as rooms might have different temperature requirements between day and night hours. We note that each device can have several inputs, which can be categorised in terms of the source of energy they consume. In particular,

- Each radiator has one input and uses heating energy.
- The blind inputs, control the positioning of the blinds, with $\boldsymbol{u}_{t,i,\text{blinds}} \in [0, 1]$, where $\boldsymbol{\xi}_{t,\text{solar}}\, u_{t,i,\text{blinds}}$ is the amount of solar radiation energy injected into the room. We assume that the electrical energy consumed by the blinds is negligible.
- TABS inject heating and cooling within certain layers of the building structure. This device is modelled as two separate inputs: the first is responsible for the heating and draws energy from the heating node, and the second is responsible for the cooling, drawing energy from the cooling node.
- AHU can affect the heating and cooling in a room by controlling the temperature of the air mass injected into the room. The dynamics of the AHU affect the temperature of the room both in a linear fashion as well as in a bilinear fashion modeling the interaction of the mixing of the air present in the room and the air injected by the AHU.

We emphasize that multiple of such devices can be present in a single building depending on its specifications. Therefore, for each building $i \in \mathcal{B}$, we can formulate the energy balance constraints as follows:

$$\left.\begin{aligned} \boldsymbol{d}_{t,i}^{\text{elect}} &= \boldsymbol{e}^\top \boldsymbol{u}_{t,i,\text{AHU}}, \\ \boldsymbol{d}_{t,i}^{\text{heat}} &= \boldsymbol{e}^\top \boldsymbol{u}_{t,i,\text{radiator}} + \boldsymbol{e}^\top \boldsymbol{u}_{t,i,\text{TABS}}, \\ \boldsymbol{d}_{t,i}^{\text{cool}} &= \boldsymbol{e}^\top \boldsymbol{u}_{t,i,\text{TABS}}, \end{aligned}\right\} \quad \forall t \in \mathcal{T}. \tag{4}$$

We close this section by defining the following constraint set for each building $i \in \mathcal{B}$:

$$\text{B}_i := \Big\{ \{\boldsymbol{d}_{t,i}\}_{t\in\mathcal{T}} : \exists \{\boldsymbol{u}_{t,i}\}_{t\in\mathcal{T}} \text{ such that (3), (4) hold} \Big\} \tag{5}$$

where

$$\begin{aligned} \boldsymbol{d}_{t,i} &= (\boldsymbol{d}_{t,i}^{\text{elect}}, \boldsymbol{d}_{t,i}^{\text{heat}}, \boldsymbol{d}_{t,i}^{\text{cool}}), \\ \boldsymbol{u}_{t,i} &= (\boldsymbol{u}_{t,i,1}, \ldots, \boldsymbol{u}_{t,i,|\mathcal{D}_i^{\text{b}}|}). \end{aligned}$$

2.1.4 Disturbances modeling

We model the disturbance $\boldsymbol{\xi}_t$ as a known deterministic forecast f_t, plus a random error $\boldsymbol{\epsilon}_t$ which we assume is a stochastic process, evolving with a known distribution. We assume that $\boldsymbol{\epsilon}_t \in [\underline{\text{eb}}_t, \overline{\text{eb}}_t]$, where $\underline{\text{eb}}_t$ and $\overline{\text{eb}}_t$ are the error lower and upper bounds, respectively. Moreover, we assume that the error terms are coupled in time. In particular, we assume that $\boldsymbol{\epsilon}_{t+1} - \boldsymbol{\epsilon}_t \in [\underline{\text{db}}_t, \overline{\text{db}}_t]$, $t = 1, \ldots, T-1$, where $\underline{\text{db}}_t$ and $\overline{\text{db}}_t$ are the time deviation lower and upper bounds, respectively. Imposing the temporal structure on vector $\boldsymbol{\xi} = (\boldsymbol{\xi}_1, \ldots, \boldsymbol{\xi}_T)$ with $\boldsymbol{\xi} \in \mathbb{R}^{k_t}$ and $k = \sum_{t\in\mathcal{T}} k_t$, the uncertainty set for the stochastic process $\{\boldsymbol{\xi}_t\}_{t\in\mathcal{T}}$ can be written as follows:

$$\Xi = \left\{ \begin{aligned} \boldsymbol{\xi} \in \mathbb{R}^k : \exists\, \boldsymbol{\epsilon}_t \in \mathbb{R}^{k_t},\ \boldsymbol{\xi}_t = f_t + \boldsymbol{\epsilon}_t, t \in \mathcal{T}, \\ \boldsymbol{\epsilon}_t \in [\underline{\text{eb}}_t, \overline{\text{eb}}_t], \qquad t \in \mathcal{T}, \\ \boldsymbol{\epsilon}_{t+1} - \boldsymbol{\epsilon}_t \in [\underline{\text{db}}_t, \overline{\text{db}}_t],\ t \in \mathcal{T}\backslash\{T\} \end{aligned} \right\}.$$

Note that in this definition of Ξ, each pair of elements $\boldsymbol{\xi}_{t,i}$ and $\boldsymbol{\xi}_{t,j}$, $i \neq j$, are assumed to be independent. In general, this assumption can be lifted by enriching Ξ with additional constraint, capturing the correlations between the different random variables.

2.2 Optimization problem

The goal of the building community is to minimize the total expected costs with respect to the electricity purchased from the grid, over a finite horizon. This must be achieved while satisfying the comfort constraint and operational constraints of the devices in the system. We assume that the cost of electricity at time t is know, and is denoted by c_t. Starting with initial conditions $\boldsymbol{x}_1 = x_1$, where x_1 is the vector containing the initial states for both the dynamical systems in the energy hub and buildings, the problem can be formulated as a multistage, bi-linear, stochastic optimization problem,

$$\begin{aligned} J(x_1) = \min\ & \mathbb{E}\left(\sum_{t\in\mathcal{T}} c_t \boldsymbol{p}_t\right) \\ \text{s.t. }\ & \boldsymbol{p}_t \in \mathcal{L}^2(\boldsymbol{I}_t),\ \boldsymbol{d}_{t,i} \in \mathcal{L}^2(\boldsymbol{I}_t),\ \forall t \in \mathcal{T},\ i \in \mathcal{B}, \\ & \big(\{\boldsymbol{p}_t\}_{t\in\mathcal{T}}, \{\boldsymbol{d}_t\}_{t\in\mathcal{T}}\big) \in \mathrm{EH}, \\ & \{\boldsymbol{d}_{t,i}\}_{t\in\mathcal{T}} \in \mathrm{B}_i,\ \forall i \in \mathcal{B}. \end{aligned} \tag{6}$$

Problem (6) is in general computationally intractable, mainly due to the non-linear dynamics in (3a). In addition, Problem (6) might be infeasible for some initial conditions. We now address these drawbacks by defining an approximation of constraint set (3) to obtain a linear multistage stochastic optimization problem. A linearized version of the bi-linear dynamics in (3a) is as follows:

$$\begin{aligned} \boldsymbol{x}_{t+1,i} = {} & A_i \boldsymbol{x}_{t,i} + B_i \boldsymbol{u}_{t,i} + C_i \boldsymbol{\xi}_t \\ & + \sum_{j\in\mathcal{D}_i^b} \left(D_{i,j}\mathbb{E}(\boldsymbol{\xi}_t) + E_{i,j} x_{1,i}\right) \boldsymbol{u}_{t,i,j}, \\ & (\boldsymbol{u}_i, \boldsymbol{\xi}) \in \mathcal{U}_i,\ \boldsymbol{u}_{t,i} \in \mathcal{L}^2(\boldsymbol{I}_t). \end{aligned} \tag{7a}$$

In particular, the bilinear terms $\boldsymbol{x}_{t,i}\boldsymbol{u}_{t,i,j}$ and $\boldsymbol{\xi}_{t,i}\boldsymbol{u}_{t,i,j}$ in (3a) are now replace with the linear terms $x_{1,i}\boldsymbol{u}_{t,i,j}$ and $\mathbb{E}(\boldsymbol{\xi}_t)\boldsymbol{u}_{t,i,j}$, respectively, where $x_{1,i}$ is the initial condition for the state of building i, and $\mathbb{E}(\boldsymbol{\xi}_t)$ denotes the expected value of $\boldsymbol{\xi}_t$. To address infeasible instances of Problem (6), we define a soft constraint formulation of the comfort constraints (3b) as follows:

$$\left.\begin{aligned}\max\{\mathrm{lb}_{t,i} - \boldsymbol{x}^{\mathrm{room}}_{t,i}, 0, \boldsymbol{x}^{\mathrm{room}}_{t,i} - \mathrm{ub}_{t,i}\} \leq \boldsymbol{s}_{t,i}.\\ \boldsymbol{s}_{t,i} \in \mathcal{L}^2(\boldsymbol{I}_t).\end{aligned}\right\} \quad \forall t \in \mathcal{T}, \tag{7b}$$

where $\boldsymbol{s}_{t,i}$ are slack variables. If the $\mathbb{E}(\boldsymbol{s}_{t,i}) = 0$, then constraints (7b) reduces to constraints (3b). If $\mathbb{E}(\boldsymbol{s}_{t,i}) > 0$, then the (3b) can be violated for some realization of $\boldsymbol{\xi}_t$. We remark that in general infeasibility may be an issue also for the energy hub constraints EH. In this case, a similar relaxation can also be applied for the constraint in EH. In the following, we assume EH is not empty for all initial conditions $\boldsymbol{x}_1 = x_1$. The linearized version of constraint set (5) is:

$$\widehat{\mathrm{B}}_i := \Big\{\{\boldsymbol{d}_{t,i}\}_{t\in\mathcal{T}},\, \{\boldsymbol{s}_{t,i}\}_{t\in\mathcal{T}} \ : \ \exists \{\boldsymbol{u}_{t,i}\}_{t\in\mathcal{T}} \quad \text{such that (4), (7) hold}\Big\}.$$

The linearized variant of Problem (6) is given as follows:

$$\begin{aligned} J(x_1) = \min\ & \mathbb{E}\left(\sum_{t\in\mathcal{T}} c_t \boldsymbol{p}_t + \gamma \sum_{t\in\mathcal{T}}\sum_{i\in\mathcal{B}} \boldsymbol{e}^\top \boldsymbol{s}_{t,i}\right)\\ \text{s.t.}\ & \boldsymbol{p}_t \in \mathcal{L}^2(\boldsymbol{I}_t),\, \boldsymbol{d}_{t,i} \in \mathcal{L}^2(\boldsymbol{I}_t), \forall i \in \mathcal{B},\, t \in \mathcal{T},\\ & \boldsymbol{s}_{t,i} \in \mathcal{L}^2(\boldsymbol{I}_t),\ \forall i \in \mathcal{B},\, t \in \mathcal{T},\\ & \big(\{\boldsymbol{p}_t\}_{t\in\mathcal{T}}, \{\boldsymbol{d}_t\}_{t\in\mathcal{T}}\big) \in \mathrm{EH},\\ & \big(\{\boldsymbol{d}_{t,i}\}_{t\in\mathcal{T}}, \{\boldsymbol{s}_{t,i}\}_{t\in\mathcal{T}}\big) \in \widehat{\mathrm{B}}_i,\ \forall i \in \mathcal{B}. \end{aligned} \tag{8}$$

The additional term $\gamma \sum_{t\in\mathcal{T}}\sum_{i\in\mathcal{B}} \boldsymbol{e}^\top \boldsymbol{s}_{t,i}$ in the objective penalizes constraint violations for the constraint set (7b), with parameter $\gamma \in \mathbb{R}_+$ providing the tradeoff between energy bought from the grid and the amount of room temperature violations. Problem (8) still retains its infinite structure involving a continuum space of decision variables and constraints. However, by taking advantage of the linear structure of the constraints and objective, in the next section we will employ well established approximation techniques which will result to finite dimensional, linear optimization problems.

2.3 Solution method

We now simplify the infinite dimensional structure of Problem (8) by restricting the infinite space of the recourse decisions $\boldsymbol{p}_t$, $\boldsymbol{d}_{t,i}$, $\boldsymbol{s}_{t,i}$ to admit a linear structure with respect to their corresponding information vector I_t. This is typically referred to a the *linear decision rule approximation*. In this setting, the structure of a policy, say $\boldsymbol{p}_t \in \mathcal{L}^2(\boldsymbol{I}_t)$, is approximated by $\boldsymbol{p}_t = p_t^\top \boldsymbol{I}_t$, where $p_t \in \mathbb{R}^{|I_t|}$. If $\boldsymbol{I}_t = (1, \boldsymbol{\xi}_1, \dots, \boldsymbol{\xi}_t)^\top \in \mathbb{R}^{t+1}$, then the structure of $\boldsymbol{p}_t$ reduces to the non-anticipative *affine policy* $\boldsymbol{p}_t = p_{t,0} + \sum_{s=1}^{t} p_{t,s}\boldsymbol{\xi}_s$. If, however, the information vector is deterministically known, e.g., $\boldsymbol{I}_t = (1) \in \mathbb{R}$, then $\boldsymbol{p}_t$ reduces to the *open-loop policy* $\boldsymbol{p}_t = p_t$. Applying linear decision rules to all recourse decisions in Problem (8), gives rise to the following optimization problem.

$$
\begin{aligned}
J(x_1) = \min\ & \mathbb{E}\left(\sum_{t\in\mathcal{T}} c_t p_t^\top \boldsymbol{I}_t + \gamma \sum_{t\in\mathcal{T}}\sum_{i\in\mathcal{B}} \boldsymbol{e}^\top S_{t,i}^\top \boldsymbol{I}_t\right) \\
\text{s.t.}\ & p_t \in \mathbb{R}^{|I_t|},\ \forall t \in \mathcal{T}, \\
& d_{t,i}^{\text{elect}}, d_{t,i}^{\text{heat}}, d_{t,i}^{\text{cool}} \in \mathbb{R}^{|I_t|},\ \forall i \in \mathcal{B},\ t \in \mathcal{T}, \\
& S_{t,i} \in \mathbb{R}^{|\text{rooms}|_i \times |I_t|},\ \forall i \in \mathcal{B},\ t \in \mathcal{T}, \\
& \left(\{p_t^\top \boldsymbol{I}_t\}_{t\in\mathcal{T}}, \{D_t \boldsymbol{I}_t\}_{t\in\mathcal{T}}\right) \in \text{EH}, \\
& \left(\{D_{t,i} \boldsymbol{I}_t\}_{t\in\mathcal{T}}, \{S_{t,i} \boldsymbol{I}_t\}_{t\in\mathcal{T}}\right) \in \widehat{\text{B}}_i,\ \forall i \in \mathcal{B},
\end{aligned}
\tag{9}
$$

where

$$
D_t = \begin{pmatrix} D_{t,1} \\ \vdots \\ D_{t,|\mathcal{B}|} \end{pmatrix},\ D_{t,i} = \begin{pmatrix} d_{t,i}^{\text{elect}\top} \\ d_{t,i}^{\text{heat}\top} \\ d_{t,i}^{\text{cool}\top} \end{pmatrix}.
$$

Problem (9) has a semi-infinite structure since it involves a finite number of decision variables p_t, D_t, S_t, $t \in \mathcal{T}$, and an infinite number of constraints due to the requirement that the constraints in EH and $\widehat{\text{B}}_i$ must hold with probability 1. Note that since all constraints are linear both with respect to the decision variables and $\boldsymbol{\xi}$, this reduces to the robust constraints that need to hold for all $\boldsymbol{\xi} \in \Xi$. Therefore, by employing linear programming duality, [3, 4], the semi-infinite constraint system can be reexpressed in terms of a finite number of linear constraints. We will denote the *robust reformulation* of EH and $\widehat{\text{B}}_i$ resulting from the linear decision rule approximation, as R-EH and R-$\widehat{\mathrm{B}}_i$, respectively, and we will refer to [4, 28] for their explicit construction. The resulting linear optimization problem can be therefore formulated as follows:

$$\begin{aligned} J(x_1) = \min \ & \sum_{t\in\mathcal{T}} c_t p_t^\top \mathbb{E}(\boldsymbol{I}_t) + \gamma \sum_{t\in\mathcal{T}} \sum_{i\in\mathcal{B}} \boldsymbol{e}^\top S_{t,i}^\top \mathbb{E}(\boldsymbol{I}_t) \\ \text{s.t.} \ & p_t \in \mathbb{R}^{|I_t|}, \ \forall t \in \mathcal{T}, \\ & d_{t,i}^{\text{elect}}, d_{t,i}^{\text{heat}}, d_{t,i}^{\text{cool}} \in \mathbb{R}^{|I_t|}, \ \forall i \in \mathcal{B}, \ t \in \mathcal{T}, \\ & S_{t,i} \in \mathbb{R}^{|\text{rooms}|_i \times |I_t|}, \ \forall i \in \mathcal{B}, \ t \in \mathcal{T}, \\ & \big(\{p_t \boldsymbol{I}_t\}_{t\in\mathcal{T}}, \{D_t \boldsymbol{I}_t\}_{t\in\mathcal{T}}\big) \in \text{R-EH}, \\ & \big(\{D_{t,i} \boldsymbol{I}_t\}_{t\in\mathcal{T}}, \{S_{t,i} \boldsymbol{I}_t\}_{t\in\mathcal{T}}\big) \in \text{R-}\widehat{\text{B}}_i, \ \forall i \in \mathcal{B}, \end{aligned}$$

where the expected values of the information sets $\mathbb{E}(\boldsymbol{I}_t)$ can be constructed since the distribution of the random variables $\boldsymbol{\xi}_t$ is assumed to be known.

We close this section by reiterating on the importance of the information structure $\boldsymbol{I}_t$ provided to the control policies. Indeed, we have already seen that if $\boldsymbol{I}_t$ contains all the primitive random variables $\boldsymbol{\xi}_t$ up to stage t, the proposed approximation reduces to the non-anticipative *affine decision rules*, while if $\boldsymbol{I}_t$ is deterministically known, the approximation produces *open-loop policies*. Another common approximation used in practice it to replace all random variables in Problem (8) with their expected value. This deterministic problem, sometimes referred to as the *certainty equivalence problem*, results in a highly scalable solution method, but does not necessarily guarantee robust constraint satisfaction. In the following section, we apply the adaptive and open-loop policies to instances of Problem (8) and compare their performance against the certainty equivalence solution method.

2.4 Numerical results

In this section, we consider a problem with 7 sources of disturbance: ambient and ground temperatures, four sources of solar radiation (North, South, East, West), and building internal gains. Historical weather and occupancy data were collected in study [49]. At each time point, and for each uncertain quantity, the data consist of a forecast f_s and a realization trajectory r_s, $s = 1, \ldots, N$, with $f_{s,t}$ denoting the forecast of stage t starting from stage s, and corresponding realization denoted by $r_{s,t}$. Remembering that in the definition Ξ, $\boldsymbol{\epsilon}_t$ denotes the error deviation from the forecast starting at time $s = 1$, the finite scenario realizations of $\boldsymbol{\epsilon}_t$ are constructed as follows:

$$\epsilon_{t,s} = r_{s,t} - f_{s,t},\ \forall s = 1, \ldots, N,\ t \in \mathcal{T},$$

with the error bounds being $\underline{\text{eb}}_t = \min\{\epsilon_{t,1}, \ldots, \epsilon_{t,N}\}$ and $\overline{\text{eb}}_t = \max\{\epsilon_{t,1}, \ldots, \epsilon_{t,N}\}$, and time deviation bounds being $\underline{\text{db}}_t = \min\{\epsilon_{t+1,1} - \epsilon_{t,1}, \ldots, \epsilon_{t+1,N} - \epsilon_{t,N}\}$ and $\overline{\text{db}}_t = \max\{\epsilon_{t+1,1} - \epsilon_{t,1}, \ldots, \epsilon_{t+1,N} - \epsilon_{t,N}\}$.

We consider an energy hub comprising 5 devices: chiller, boiler, heat pump (HP), photovoltaics (PV), battery. We model the chiller, boiler and heat pump using a coefficient of performance [16], which gives rise to the following constraints.

$$\left.\begin{aligned} \boldsymbol{u}^{\text{out}}_{t,\text{chiller}} &= 0.7\boldsymbol{u}^{\text{in}}_{t,\text{chiller}}, \\ \boldsymbol{u}^{\text{out}}_{t,\text{boiler}} &= 0.7\boldsymbol{u}^{\text{in}}_{t,\text{boiler}}, \\ \boldsymbol{u}^{\text{out}}_{t,\text{HP}} &= 3\boldsymbol{u}^{\text{in}}_{t,\text{HP}}, \end{aligned}\right\} \quad \forall t \in \mathcal{T}.$$

All three devices are assumed to have infinite capacity, with $\boldsymbol{u}^{\text{in}}_t, \boldsymbol{u}^{\text{out}}_t \geq 0$ for all $t \in \mathcal{T}$. We consider a photovoltaic array with maximum output of 8.02kW, which is modelled using the following linear constraints [18] that depend linearly on the ambient temperature, and the solar radiation (South):

$$0 \leq \boldsymbol{u}^{\text{out}}_{t,\text{PV}} \leq 0.1655 - 0.0066\boldsymbol{\xi}_{t,\text{Amb.Temp.}} + 7.8\boldsymbol{\xi}_{t,\text{Solar(S)}},$$

for all $t \in \mathcal{T}$. Note that the units of $\boldsymbol{\xi}_{t,\text{Solar(S)}}$ are measured in kW/m^2 and can typically take values $\boldsymbol{\xi}_{t,\text{Solar(S)}} \in [0, 1]$. Finally, we consider a lead-acid battery [56], with a 5kW

Building specifications

No.	Area(m^2)	WFA	BT	CT	Input Devices
1	420	30%	SP	heavy	AHU, blinds, radiator
2	228	50%	SP	light	AHU, blinds, TABS
3	276	80%	SA	light	AHU, blinds, TABS
4	516	50%	SA	heavy	AHU, blinds, radiator
5	324	50%	SP	heavy	AHU, blinds, radiator

Table 1: *Summary of the* 5 *buildings used in the simulations.*

capacity, giving rise to the following linear dynamical system:

$$\left.\begin{aligned} \boldsymbol{x}_{t+1} = &\begin{pmatrix} 0.51 & 0.22 \\ 0.47 & 0.78 \end{pmatrix} \boldsymbol{x}_t \\ &+ \begin{pmatrix} 0.61 \\ 0.25 \end{pmatrix} \boldsymbol{u}_t^{\text{in}} + \begin{pmatrix} -0.83 \\ -0.39 \end{pmatrix} \boldsymbol{u}_t^{\text{out}}, \end{aligned}\right. \quad \forall t \in \mathcal{T},$$

where the states and control are constrained by:

$$\left.\begin{aligned} &0 \leq \boldsymbol{u}_t^{\text{in}}, \boldsymbol{u}_t^{\text{out}} \leq 8, \\ &1 \leq \boldsymbol{x}_{t,1} + \boldsymbol{x}_{t,2} \leq 5, \; 0 \leq \boldsymbol{x}_t, \\ &0.62\boldsymbol{x}_{t,1} + 0.27\boldsymbol{x}_{t,2} - \boldsymbol{u}_t^{\text{out}} \geq 0, \\ &0.84\boldsymbol{x}_{t,1} + 0.37\boldsymbol{x}_{t,2} + \boldsymbol{u}_t^{\text{in}} \leq 2.58, \\ &0.73\boldsymbol{x}_{t,1} + 0.73\boldsymbol{x}_{t,2} + \boldsymbol{u}_t^{\text{in}} \leq 3.66. \end{aligned}\right\} \quad \forall t \in \mathcal{T}.$$

The dynamics and constraints of each building, given in (3), are generated using the BRCM toolbox [50]. In particular, we use building models described in [49], with their main features summarised in Table 1. All building consists of 5 zones with unique zone areas. The total area of the building is reported in the second column. Each building is characterised by the building type BT $\in$ {Swiss Passive (SP), Swiss Average(SA)}, and construction type CT = {heavy, light}. Moreover, each building is decomposed into zones, which are characterized by a window fraction area WFA = $\{30\%, 50\%, 80\%\}$ and their corresponding facade orientation. Finally, the BRCM toolbox is provided with the individual building construction details along with the specification of the control devices (radiators, AHU, TABS, blinds).

Time	c_t	lb_t	ub_t
05:00 - 23:00	0.145CHF	21°C	25°C
23:00 - 05:00	0.097CHF	15°C	30°C

Table 2: *Electricity day/night tariff variations and comfort constraints bounds.*

The following computation experiments compare the performance of affine decision rules (ADR), open-loop policies (OLP) and the certainty equivalent problem (CEP), for a problem instance with $T = 12$, $\gamma = 10^3$. All problems assume time-varying electricity tariffs and comfort constraints given in Table 2. Note that the electricity prices c_t, are given in Swiss Franc (CHF) and the same comfort bounds lb_t, ub_t are used in all rooms and all buildings considered in the system. The performance of the system is evaluated on a receding horizon implementation of the system, i.e., the first input resulting from the corresponding approximation of Problem (9) together with the disturbance realizations are applied to the *original nonlinear system dynamics* (3a), and the next state is evaluated. The procedure is repeated in a receding horizon fashion for a time horizon of 1 week. The system was simulated using data realizations of 8 consecutive weeks (restarting at the beginning of each week) for the winter and summer periods of 2007, starting January 1st and June 29th, respectively. Table 2 reports the statistics from these simulation results, with the cost being measured in Swiss Francs (CHF) and comfort constraint violations measured in kelvin hours (Kh), and the entries correspond to (mean,standard deviation) over the scenarios considered. We observe that the certainty equivalent approximation produces the least cost at the expense of large constraint violations both for the winter and summer periods. The robust approximations (open-loop and affine policies), produce higher costs but with much lower constraint violations. The negative performance of the certainty equivalent approximation with respect to the constraint violations can be explained in two ways: (i) the approximation assumes a deterministic evolution of the uncertain parameters, which results in frequent constraint violations since the system pushes the states close to the comfort constraints in order to minimize the electricity cost, however, when an unaccounted disturbance is realized, the next state ends up being outside the comfort constraints. Moreover, the model mismatch between the linear dynamics (7a) and the actual bi-linear dynamics (3a), reduce the predictive capabilities of Problem (8). In contrast, the robust approximations fully incorporate the stochastic evolution of uncertaint parameters but suffer slightly from the linearization of the system's dynamics. We note that the slightly more constraint violations of the open-loop polices compared to affine decision rules can be attributed to the non-adaptive nature of the open-loop policies. The inability of open-loop policies to adapt can potentially lead to greater difficulty in satisfying the robust constraints and thus lead to undesired constraint violations. Finally, for each step in the receding horizon, certainty equivalent problem and open-loop policies are solved within 2 second, while affine decision rules require approximate 15 seconds.

	Winter	
Method	Cost (CHF)	Violation (Kh)
CEP	$(34.0, 2.2)$	$(30.4, 1.5)$
OLP	$(48.7, 1.7)$	$(5.6, 0.5)$
ADR	$(44.2, 1.1)$	$(5.5, 0.4)$

	Summer	
Method	Cost (CHF)	Violation (Kh)
CEP	$(1.5, 0.3)$	$(7.4, 2.0)$
OLP	$(5.2, 0.4)$	$(2.7, 0.6)$
ADR	$(4.7, 0.5)$	$(1.5, 0.4)$

Table 3: *Receding horizon simulations.*

To better understand the behaviour of the three approximations, the trajectories for the state of the battery charge, room temperature in the first room in building 1, and the total energy purchased from the grid $\boldsymbol{p}_t$, are depicted Figure 2. The results verify the behaviour of the three control strategies. Indeed, the certainty equivalent approximation operates very near to the comfort constraint and leads to frequent constraint violations, while the robust approximation produces more conservative results, keeping the room temperature well inside the comfort range at the expense of more energy consumption. All three approximation fully utilize the load shifting capabilities of the battery, storing energy during the evening hours when electricity is cheaper, and deploying that energy in the early morning hours when the building needs to be brought back within the comfort range. From these results, we conclude that the adaptive nature of the affine decision rules produces a good compromise between the optimistic decisions made by the certainty equivalent approximation and the over conservative decisions of the open-loop policies.

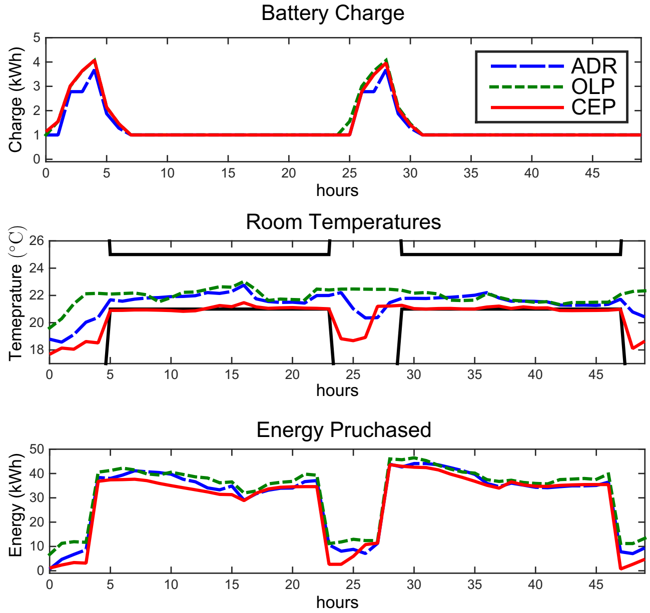

Figure 2: *Profile trajectories for the state of the battery charge (top), room temperature in the first room in building* 1 *(center), and the total energy purchased from the grid (bottom). The battery charge is calculated as the sum of the two states appearing in* (2.4). *The black lines in second graph correspond to the comfort constraint. The uncertain data correspond to the winter period, with the ambient temperature ranging around* $5°C$.

2.5 Conclusion

In this chapter, we presented a unified framework for controlling the operation of the energy hub and the buildings it connects, and formulated a optimization problem that ensures the energy needs of the buildings are met with the minimum cost. We used a decision rule approximation for solving the resulting infinite-dimensional stochastic problem. Our simulations which are based on realistic data have demonstrated that the adaptive nature of the affine decision rules produce a good trade-off between energy consumption and comfort violation compared to established solution techniques.

Future work concentrates on a more comprehensive modeling of the energy hub's dynamics, as well as considering larger building communities connected to the energy hub. From a practical prospective, this will require to investigate the impact of more flexible policies for further reducing the conservativeness of affine decision rules, as well as exploiting the naturally decomposable nature of the problem by implementing distributed and decentralized control schemes.

3 Tractable Approximation of Chance-Constrained Systems via Piecewise Affine Policies

Robust Model Predictive Control (MPC) is a popular methodology to design controllers for constrained uncertain systems subject to input and state constraints [27, 46, 35]. The resulting control law guarantees constraint satisfaction for all possible disturbance realizations. Although successful in many cases, this method may lead to “conservative" controllers with poor performance, since only the support of the disturbance is taken into account, but not its distribution. In fact, it is often the “unlikely" disturbances that tend to limit the performance of Robust MPC.

Chance-constrained Stochastic MPC (SMPC) is an alternative modeling paradigm in which the constraints are interpreted probabilistically, allowing them to be violated for “unlikely" disturbances [39, 11, 12, 13]. Unfortunately, chance-constrained SMPC problems are notoriously hard to solve computationally for two main reasons: (*i*) They involve a continuum space of decision variables, and (*ii*) Chance constraints are in general non-convex and require the computation of multi-dimensional integrals. A popular approximation for addressing (*i*) is to restrict the set of admissible policies to those possessing a simple functional form, such as affine or piecewise affine (PWA) policies [25, 31, 24], reducing the resulting problem to a static chance-constrained problem with finitely many decision variables. A popular approach to address (*ii*) is to use randomized algorithms, and in particular the "scenario approach" [10, 7]. These algorithms replace the chance constraint by a finite set of sampled constraints, and result in a convex optimization problem whose size grows polynomially with respect to the input data.

Randomized MPC (RMPC) algorithms based on the “scenario approach" have been successfully used in the context of chance-constrained SMPC [43, 53, 6, 44, 62, 42], since the method is independent of the underlying probability distribution that describes the uncertainty. Nevertheless, even for simple policy structures such as affine policies, RMPC tends to produce conservative results, both in terms of objective value and constraint violation probability [60]. The application of non-linear policies towards RMPC may partly alleviates this drawback at the expensive of a significant increase in the problem size [53].

The goal of this paper is to propose an alternative approach to the standard RMPC algorithms studied in [43, 53, 6, 44, 62, 42], and is based on recent results of [34, 60]. The proposed method combines the ideas from randomized algorithms, robust optimization and piecewise affine (PWA) policies. The method allows us to efficiently exploit the increased flexibility of non-linear policies, therefore reducing the cost of the resulting optimization problem. In particular, we will show that the number of constraints in the resulting optimization problem is by a factor of $\mathcal{O}(N/\epsilon)$ smaller than in standard RMPC, while requiring $\mathcal{O}(pN)$ fewer samples, where p is the desired complexity of the PWA policy. Numerical simulations show that the proposed approach can effectively address both conservatism of the solution as well as high computation time associated with standard RMPC approaches. In fact, we show that we are able to solve problem instances orders of magnitude faster than standard RMPC approaches with affine policies, while reducing cost. Note that this paper is concerned with efficiently solving the chance-constrained optimization problem arising in the SMPC approach. Other aspects of SMPC, such as stability and recursive feasibility, are subject to further research.

The paper is organized as follows: Following the brief literature review next, we formulate the chance-constrained SMPC problem in Section 3.2. Section 3.3 summarizes the standard RMPC approach with PWA policies. We describe the proposed methodology in Section 3.4, whereas Section 3.5 discusses numerical results on an inventory control problem. Section 3.5.4 concludes the paper.

3.1 Related Literature

Randomized algorithms (also known as Monte-Carlo methods) have been successfully used for approximating chance-constrained optimization problems [21, 22, 32, 40, 37, 9, 10, 7, 51, 52, 55, 54]. One approach is based on the Vapnik-Chervonenkis (VC) theory of statistical learning theory [52, 55, 54], which can in principle be applied to all problems with finite VC-dimension, even if the underlying constraint functions are non-convex. Unfortunately, it is widely accepted that VC-theory comes with high sample sizes, resulting in conservative solutions [8, Section 1.2]. Recently, a new randomized method known as the “scenario approach" has emerged [10, 7]. Compared to methods based on the theory of statistical learning theory, the sample sizes required by the scenario approach are typically much lower [7, Section 10], while compared to other randomization-based methods [21, 22, 32, 40, 37, 52, 55, 54], the scenario approach is distribution-free and applies to any chance-constrained problem whose underlying functions are convex.

Recently, considerable effort has been spent on reducing the sample size for scenario optimization problems [45, 58, 59, 34, 60]. Roughly speaking, [45, 58, 59] show that if the constraint functions exhibit special structural properties (e.g. affine in the decision and/or uncertainty variable), then it might be possible to improve the sample samples. A slightly different way of applying the scenario approach is described in [60, 34], where the authors approximate the uncertainty set by “box" containing $(1-\epsilon)$ of the total probability mass, and then solve a robust optimization problem with respect to this box. This approach outperforms the standard scenario approach in terms of computational efficiency, at the expense of typically producing more conservative solutions. To address the latter issue, the present paper proposes the use of more flexible policies while keeping the computational advantage.

3.2 Problem Description

3.2.1 Dynamics, constraints and control objective

We consider discrete-time linear systems of the form

$$x_{k+1} = Ax_k + Bu_k + Ew_k, \tag{10}$$

where $k \in \{0, \dots, N-1\}$ is the time index, N is the prediction horizon, $x_k \in \mathbb{R}^{n_x}$ is the state, $u_k \in \mathbb{R}^{n_u}$ is the input, and A, B and E are (known) system matrices. At each time step, the system is affected by a random disturbance $w_k \in \mathbb{R}^{n_w}$. Furthermore, we consider linear state and input constraints of the form:

$$Gu_k \le g, \qquad Fx_{k+1} \le f, \tag{11}$$

for matrices $G \in \mathbb{R}^{n_g \times n_f}$, $g \in \mathbb{R}^{n_g}$, $F \in \mathbb{R}^{n_f \times n_x}$, and $f \in \mathbb{R}^{n_f}$, where n_f (n_g) is the number of state (input) constraints. For simplicity we assume that $\mathbb{U} := \{u \in \mathbb{R}^{n_u} : Gu \leq g\}$ and $\mathbb{X} := \{x \in \mathbb{R}^{n_x} : Fx \leq f\}$ are compact sets with non-empty relative interior. Let us now compactly rewrite system (10) and constraints (11) in the form:

$$\mathbf{x} = \mathbf{A}x + \mathbf{B}\mathbf{u} + \mathbf{E}\mathbf{w}, \qquad (12)$$
$$\mathbf{G}\mathbf{u} \leq \mathbf{g}, \qquad \mathbf{F}\mathbf{x} \leq \mathbf{f},$$

where $\mathbf{x} := [x_1, \ldots, x_N] \in \mathbb{R}^{Nn_x}$ is the predicted state sequence, x is the (known) initial state, $\mathbf{u} := [u_0, \ldots, u_{N-1}] \in \mathbb{R}^{Nn_u}$ is the input sequence, and $\mathbf{w} := [w_0, \ldots, w_{N-1}] \in \mathbb{R}^{Nn_w}$ is the disturbance sequence. The matrices $\mathbf{A}$, $\mathbf{B}$, $\mathbf{E}$, $\mathbf{G}$, $\mathbf{g}$, $\mathbf{F}$, and $\mathbf{f}$ can be easily constructed from the problem data in (10) and (11).

In this paper, we assume that $\mathbf{w}$ is a random variable defined on a probability space ($\mathbb{W}$, $\mathcal{F}$, $\mathbb{P}$). We further assume that its support $\mathbb{W} \subset \mathbb{R}^{Nn_w}$ is a known compact polyhedron with non-empty interior. In contrast, the distribution $\mathbb{P}$ does not need to be known explicitly, but we require that independent samples of the form $\{\mathbf{w}^{(1)}, \mathbf{w}^{(2)}, \ldots\}$ can be drawn according to $\mathbb{P}$. In practical applications, such samples can be obtained from historical data, while the support $\mathbb{W}$ can be (conservatively) estimated from the data. Note that due to their dependences on $\mathbf{w}$, the states $\mathbf{x}$ become random variables as well. This allows us to model the state constraints in (12) probabilistically as chance constraints in the form

$$\mathbb{P}[\mathbf{F}\mathbf{x} \leq \mathbf{f}] \geq 1 - \epsilon. \qquad (13)$$

Remark 1 *This paper considers joint chance constraints of the form* (13)*, where we require the entire state trajectory* $\mathbf{x}$ *to lie inside* $\mathbb{X}^N$ *with probability* $1 - \epsilon$*. However, in certain applications it is more natural to address individual chance constraints of the form* $\mathbb{P}[Fx_k \leq f] \geq 1 - \epsilon$*,* $k = 1, \ldots, N$*, see e.g. [58, 44]. Nevertheless, all subsequent results can be extended to individual chance constraints in a natural way.* □

The objective is to compute a control law which minimizes the expected value of a convex cost function given by

$$J(\mathbf{u}) = \mathbb{E}\left[\sum_{k=0}^{N-1} \ell(x_k, u_k) + \ell_f(x_N)\right], \tag{14}$$

where $\ell : \mathbb{R}^{n_x} \times \mathbb{R}^{n_u} \to \mathbb{R}$ is a convex stage cost, $\ell_f : \mathbb{R}^{n_x} \to \mathbb{R}$ is a convex terminal cost, and $\mathbb{E}[\cdot]$ is the expectation with respect to $\mathbb{P}$.

3.2.2 Optimization over feedback policies

In its most general setting, the control problem consists of finding a (measurable) feedback policy $\Pi := [\pi_0, ..., \pi_{N-1}]$,

$$\pi_k : (w_0, \ldots, w_{k-1}) \mapsto u_k := \pi_k(w_0, \ldots, w_{k-1}), \tag{15}$$

which minimizes the cost in (14) subject to state and input constraints. Intuitively speaking, the advantage of using “closed-loop" (i.e., feedback) policies compared to the “open-loop" policy, where $\mathbf{u}$ is treated as a static variable, is that the former is able to account for disturbances $\mathbf{w}$ entering the system [35]. Note that in (15) we restrict ourselves to strictly causal policies, whereas in certain applications causal policies of the form $\pi_k : (w_0, \ldots, w_k) \mapsto u_k := \pi_k(w_0, \ldots, w_k)$ are more natural. However, all the following discussions apply to causal policies as well, with only minor changes.

3.2.3 Chance-constrained Stochastic MPC formulation

The chance-constrained Stochastic MPC problem is now obtained by combining (13)–(15), and is given by

$$\begin{aligned} \min_{\mathbf{u}\in\Pi} \quad & J(\mathbf{u}) && \text{(ccSMPC)} \\ \text{s.t.} \quad & \mathbf{G}\mathbf{u} \leq \mathbf{g}, \qquad \forall \mathbf{w} \in \mathbb{W}, \\ & \mathbb{P}\left[\mathbf{F}\left(\mathbf{A}x + \mathbf{B}\mathbf{u} + \mathbf{E}\mathbf{w}\right) \leq \mathbf{f}\right] \geq 1 - \epsilon. \end{aligned}$$

Note that in (ccSMPC) we allow state constaints to be violated with probability ϵ, whereas the input constraints must be satisfied for every possible uncertainty realization $\mathbf{w} \in \mathbb{W}$.

Recall that due to the chance constraint, the feasible region of (ccSMPC) is non-convex in general.

The goal of this paper is to present tractable and computationally efficient approximation methods for solving (ccSMPC). In Section 3.3, we first review the standard method of approximating (ccSMPC) using randomization and PWA policies. As we will see, this method results in large (albeit convex) problems which are typically computationally expensive to solve. We address this issue in Section 3.4.2, where we first formulate an infinite dimensional convex problem that conservatively approximates (ccSMPC), and then further approximate the resulting problem using PWA policies.

3.3 Randomized MPC with Piecewise Affine Policies

In general, (ccSMPC) is computationally intractable to solve because (i) it involves the optimization over the infinite-dimensional space of all measurable functions, and (ii) the chance constraints render the problem non-convex. A popular approach to obtain a tractable approximation of (ccSMPC) is to first restrict the function space of admissible policies Π, and then use randomized algorithms to approximate the resulting (static) chance constraint [43, 53, 6, 44, 58]. This section briefly recalls this strategy and lays the foundation for subsequent discussion.

3.3.1 Piecewise affine (PWA) policies

We deal with problem (i) by restricting Π to a class of policies first introduced in [24, Section 4.1], which take the form

$$\mathbf{u} = \mathbf{H}\, L(\mathbf{w}) + \mathbf{h}. \tag{16}$$

Here, $\mathbf{H} \in \mathbb{R}^{Nn_u \times Npn_w}$ and $\mathbf{h} \in \mathbb{R}^{Nn_u}$ are design variables, and $L : \mathbb{R}^{Nn_w} \to \mathbb{R}^{Npn_w}$ is a nonlinear "lifting" operator that dictates the structure of the policies. In particular, we will use the definition of the piecewise linear operator $L(\cdot)$ given in [24, eq. (3)], with $p \geq 1$ defining the number of affine pieces. Note that if $L(\mathbf{w}) = 0$ for all $\mathbf{w}$, then (16) corresponds to open-loop policies, while if $L(\cdot)$ is the identity map, then (16) correspond to affine policies.

The parameter p defines the number of *partitions* in the PWA policy as well as the number of decision variables in $\mathbf{H}$. Therefore, it can be interpreted as the "complexity" parameter associated with (16). An one-dimensional example with $p \in \{1, 2, 3\}$ is provided in Fig. 3. As it can be seen there, p is the parameter defining the maximum number of affine pieces. In the interest of space, we do not describe the lifting approach in more detail, but refer the interested reader to [24] for details.

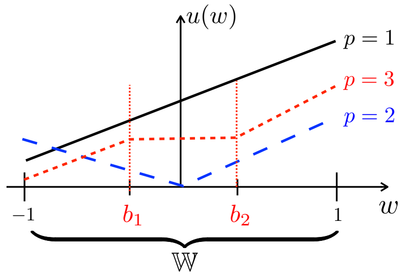

Figure 3: *One-dimensional illustration of PWA policy* (16) *with different number of partitions of same length:* $p = 1$ *(solid black line),* $p = 2$ *(dashed blue line), and* $p = 3$ *(dotted red line). The variables* b_1 *and* b_2 *are "break points" and define the shape of the partitions (here for* $p = 3$*).*

Policies of the general form (16) are computationally attractive because the resulting optimization problem has a finite number of decision variables [24, 53]. Unfortunately, the chance constraint in (ccSMPC) renders the optimization problem non-convex and thus computationally intractable to solve.

3.3.2 Sample approximation of chance constraint

One way of approximating chance constraints is by means of randomization, and is based on the "scenario approach" introduced in [9, 10, 7]. The idea is to replace the chance constraint in (ccSMPC) with a finite number of randomly sampled constraints [43, 53, 6, 44, 62].

More precisely, let $\{\mathbf{w}^{(1)}, \ldots, \mathbf{w}^{(S)}\} \subset \mathbb{R}^{Nn_w}$ be a collection of independent samples drawn according to $\mathbb{P}$. Then, the Randomized MPC (RMPC) problem subject to the PWA policy

(16) is given by

$$\begin{aligned} \min_{\mathbf{H},\mathbf{h}} \quad & J(\mathbf{H},\mathbf{h}) \\ \text{s.t.} \quad & \mathbf{G}(\mathbf{H}\,L(\mathbf{w})+\mathbf{h}) \leq \mathbf{g}, \qquad \forall \mathbf{w} \in \mathbb{W}, \\ & \mathbf{F}\left(\mathbf{A}x + \mathbf{B}\left(\mathbf{H}\,L(\mathbf{w}^{(i)})+\mathbf{h}\right) + \mathbf{E}\mathbf{w}^{(i)}\right) \leq \mathbf{f}, \\ & \text{for all } i = 1,\dots,S. \end{aligned} \tag{RMPC(p)}$$

If, for a fixed value $\beta \in (0,1)$, the sample size S satisfies

$$\sum_{j=0}^{\zeta-1} \binom{S}{j} \epsilon^j (1-\epsilon)^{S-j} \leq \beta, \tag{17}$$

then, under certain (non-restrictive) technical assumptions[1], the solution of RMPC(p) will be feasible to (ccSMPC) with probability at least $1-\beta$, where ζ is the number of decision variables in RMPC(p). Intuitively speaking, the parameter $\beta \ll 1$ upper bounds the probability that the solution of RMPC(p) will not satisfy the chance constraint in (ccSMPC), and can in practice chosen to be arbitrarily close to 0. An explicit upper bound on the sample size S was established in [7], and is given by

$$S \geq \frac{2}{\epsilon}\Big(\zeta - 1 + \ln\frac{1}{\beta}\Big).$$

Note that the number of decision variables in RMPC(p) is $\zeta = Nn_u + n_u p n_w \frac{N(N-1)}{2}$. Therefore, the required sample size S grows quadratically in N and linearly in p. In addition, for fixed n_u and n_w, RMPC(p) involves $\mathcal{O}(pN^2)$ decision variables and $\mathcal{O}(pN^3/\epsilon)$ constraints[2]. Although convex, the large number of constraints often limits the applicability of RMPC for practical problems. As reported in [60], even for affine policies with $p = 1$, only problems of modest sizes (e.g. $n_w = 1$, $n_u = 1$, and $N \leq 20$) can be solved efficiently.

The next section aims to alleviate this drawback by proposing a method which results in optimization problems that grow only $\mathcal{O}(pN^2)$ with respect to both the number of decision

[1] Typically these assumptions include convexity, uniqueness of optimizer and i.i.d. sampling. We refer the interested reader to [9] for the full exposition.

[2] Recall that $\mathbf{F}$ is a matrix of dimension $Nn_f \times Nn_x$, which is replicated S-times in RMPC(p)

variables and constraints.

Remark 2 *We note that in case individual chance constraints of the form $\mathbb{P}[Fx_k \leq f] \geq 1-\epsilon$, $k = 1, \ldots, N$, are considered, then the sample sizes can be improved. In the interest of space, we omit the details but refer the interested reader to [58, 59, 44] for the details.*

3.4 Proposed "Box-Approach"

The proposed algorithm is an extension of the results of [34, 60] to PWA policies, and is based on a combination of randomized and robust optimization. Conceptually speaking, the proposed approach reverses the two approximation steps of Section 3.3, by first using the scenario approach to construct a set that contains $(1-\epsilon)$ of the probability mass of $\mathbf{w}$ and formulate an infinite dimensional convex (inner) approximation of (ccSMPC), and then approximate the resulting infinite dimensional problem using policies. The key observation enabling this method is based on the observation that *any feasible input policy* is guaranteed to satisfy the original chance constraint with high confidence (Theorem 1 below). As will be shown in Section 3.4.3, the resulting optimization problem is smaller than RMPC(p) by a factor of $\mathcal{O}(N/\epsilon)$ in terms of constraints, while requiring fewer samples.

3.4.1 Bounding the uncertainty

Following [34], we first seek a set $\mathbb{B} \subset \mathbb{R}^{Nn_w}$ that satisfies the condition $\mathbb{P}[\mathbf{w} \in \mathbb{B}] \geq 1-\epsilon$. For simplicity, we assume that $\mathbb{B}$ is a "box", i.e., an axis-aligned hyper rectangle[3] parametrized by its (component-wise) upper and lower bounds $\underline{\gamma}, \overline{\gamma} \in \mathbb{R}^{Nn_w}$. Consider now the following chance-constrained problem,

$$\begin{aligned} \min_{\underline{\gamma},\overline{\gamma}} \quad & \left\|\overline{\gamma} - \underline{\gamma}\right\|_1 \\ \text{s.t.} \quad & \mathbb{P}\left[\mathbf{w} \in [\underline{\gamma}, \overline{\gamma}]\right] \geq 1-\epsilon, \end{aligned} \tag{18}$$

[3] The choice of a hyper-rectangle is not restrictive; any other geometric representation with a finite dimensional convex parametrization, such as an ellipsoid, could have been chosen instead.

whose solution provides an appropriate parametrization for the construction of the set $\mathbb{B}$. We solve the chance-constrained optimization problem (18) by means of randomization:

$$\begin{aligned} \min_{\underline{\gamma},\overline{\gamma}} \quad & \|\overline{\gamma} - \underline{\gamma}\|_1 \\ \text{s.t.} \quad & \underline{\gamma} \le \mathbf{w}^{(i)} \le \overline{\gamma}, \quad i = 1, \dots, S\text{-B}, \end{aligned} \tag{19}$$

where S-B is chosen according to (17) with $\zeta = 2Nn_w$. We remark that problem (19) can be solved analytically by taking the element-wise maximum and minimum of the extracted samples for $\underline{\gamma}$ and $\overline{\gamma}$, respectively. If $\mathbb{B}$ is the box corresponding to the optimal solution of (19), then it follows from [10, Theorem 1] that $\mathbb{P}^{S\text{-B}}\big[\mathbb{P}[\mathbf{w} \notin \mathbb{B}] \le \epsilon\big] \ge 1 - \beta$.

3.4.2 Convex inner approximation

Consider now the following convex (inner) approximation of (ccSMPC):

$$\begin{aligned} \min_{\mathbf{u}\in\Pi} \quad & J(\mathbf{u}) \\ \text{s.t.} \quad & \mathbf{G}\mathbf{u} \le \mathbf{g}, \qquad \forall \mathbf{w} \in \mathbb{W}, \\ & \mathbf{F}\left(\mathbf{A}x + \mathbf{B}\mathbf{u} + \mathbf{E}\mathbf{w}\right) \le \mathbf{f}, \quad \forall \mathbf{w} \in \mathbb{B} \cap \mathbb{W}. \end{aligned} \tag{20}$$

Note that the original chance constraint is now replaced by a robust constraint which needs to be satisfied for all uncertainty realizations of $\mathbb{B} \cap \mathbb{W}$. It is easy to see that, in contrast to (ccSMPC), problem (20) is *convex*. The following Theorem formally establishes the connection between the two problems.

Theorem 1 *For all $\epsilon, \beta \in (0,1)$, assume that S-B satisfies* (17) *with $\zeta = 2Nn_w$. Then, with confidence no smaller than $1-\beta$, any feasible policy in* (20) *is feasible to* (ccSMPC).
□

Proof The proof follows closely that of [34, Prop. 1], and is provided in Appendix **??** for completeness.

In other words, with confidence at least $1-\beta$, the feasible set of problem (20) constitutes a *convex inner approximation* of the feasible set of (ccSMPC). Unfortunately, problem (20) still remains intractable as it requires the optimization over the space of all (measurable) functions Π. Similar to Section 3.3, a tractable approximation can be obtained by restricting the function space Π to policies of the form (16):

$$
\begin{aligned}
\min_{\mathbf{H},\mathbf{h}}\ & J(\mathbf{H},\mathbf{h}) && \text{(RMPC-B}(p))\\
\text{s.t. } & \mathbf{G}(\mathbf{H}\,L(\mathbf{w})+\mathbf{h}) \le \mathbf{g}, && \forall \mathbf{w}\in\mathbb{W},\\
& \mathbf{F}\left(\mathbf{A}x+\mathbf{B}\left(\mathbf{H}L(\mathbf{w})+\mathbf{h}\right)+\mathbf{E}\mathbf{w}\right) \le \mathbf{f}, && \forall \mathbf{w}\in\mathbb{B}\cap\mathbb{W}.
\end{aligned}
$$

Corollary 1 *For all $\epsilon,\beta\in(0,1)$ and $p\ge 1$, assume that S-B satisfies* (17) *with $\zeta = 2Nn_w$. Then, with confidence no smaller than $1-\beta$, any feasible solution in* RMPC-B(p) *is feasible in* (ccSMPC). □

For the PWA policies considered, the semi-infinite structure of RMPC-B(p) can be reformulated exactly as a linear program that involves $\mathcal{O}(pN^2)$ decision variables and $\mathcal{O}(pN^2)$ constraints. We refer the interested read to [24] for details about the reformulation.

3.4.3 Complexity of RMPC(p) and RMPC-B(p)

The RMPC(p) and RMPC-B(p) approaches differ mainly in two points: (i) The sample sizes S and S-B required to ensure that the optimal solutions of RMPC(p) and RMPC-B(p) are feasible to (ccSMPC), and (ii) The size of the resulting optimization problem to be solved. We have already seen that the sample size required by RMPC(p) grows quadratically in N and linearly in p, while the corresponding sample size required by RMPC-B(p) grows only linearly in N and is independent of p. The latter follows since the number of decision variables in (19) is $2Nn_w$. It can be verified that, for fixed n_u and n_w, RMPC(p) involves $\mathcal{O}(pN^2)$ decision variables and $\mathcal{O}(pN^3/\epsilon)$ constraints, while RMPC-B(p) involves only $\mathcal{O}(pN^2)$ decision variables and $\mathcal{O}(pN^2)$ constraints. For fixed problem data n_u and n_w, these complexity results are summarized in Table 4 as functions of the parameters N, ϵ, and p. Table 4 clearly shows that, from a computational point of view, RMPC-B(p) can be solved more efficiently than RMPC(p), as the corresponding optimization problem features a factor of $\mathcal{O}(N/\epsilon)$ fewer constraints. Its effect on computation time is demonstrated in an example in the following section.

Table 4: *Complexity analysis between RMPC(p) and RMPC-B(p)*

Method	# decision variables	# constraints	# samples
RMPC	$\mathcal{O}(pN^2)$	$\mathcal{O}(pN^3/\epsilon)$	$\mathcal{O}(pN^2/\epsilon)$
RMPC-B	$\mathcal{O}(pN^2)$	$\mathcal{O}(pN^2)$	$\mathcal{O}(N/\epsilon)$

3.5 Numerical Example

In this section, we compare the performance of RMPC(p) and RMPC-B(p). In particular, we consider an inventory control problem whose dynamics evolve as:

$$x_{k+1} = x_k + u_k - w_k, \qquad x_0 = 350,$$

for $k = 0, \ldots, N-1$. Here $x_k \in \mathbb{R}$ represents the state of inventory level of the warehouse, $u_k \in \mathbb{R}$ is the production level of the factory, and $w_k \in \mathbb{R}$ models the uncertain demand. We assume that the uncertain demands $w_k \in [0, 100]$ are i.i.d. random variables that follow a truncated normal distribution with mean 50 and standard deviation 10. At each time step, we require the inventory level to lie between 0 and 1000 with probability at least $1-\epsilon$, and the initial inventory level is $x_0 = 350$. The objective is to minimize the average production cost over the planning horizon. This gives rise to the following instance of (ccSMPC).

$$\begin{aligned}
\min_{\mathbf{u}\in\Pi} \quad & \mathbb{E}[\mathbf{1}^\top \mathbf{u}] \qquad (21)\\
\text{s.t.} \quad & \mathbf{u} \geq 0, \quad \forall \mathbf{w} \in \mathbb{W},\\
& \mathbb{P}\left[0 \leq x_k \leq 1000,\, k = 1, \ldots, N\right] \geq 1-\epsilon,\\
& x_{k+1} = x_k + u_k - w_k, \quad k = 0, \ldots, N-1,\\
& x_0 = 350,
\end{aligned}$$

where $\mathbf{1} \in \mathbb{R}^N$ is a vector containing all ones, and the control inputs are assumed to be causal as described in Section 3.2.2.

In the following, we conduct three numerical comparisons: (*i*) We compare the sample size needed to guarantee that the two approximation methods RMPC(p) and RMPC-B(p) are probabilistically feasible to problem (21); (*ii*) We compare the solution time and computational resources needed by the two methods; and (*iii*) We compare the performance and the empirical violation probability of each method.

3.5.1 Sample sizes

For this numerical study we fix $\epsilon = 0.1$ and $\beta = 10^{-7}$, and consider PWA policies with $p \in \{1, 4, 8\}$ and horizon $N = 10, \ldots, 60$. Table 5 lists the number of samples required for both approaches to be probabilistically feasible in (21). These sample sizes are obtained by numerically inverting (17).

It can be seen that S-B, the sample size associated with RMPC-B, is much smaller compared to S, associated to RMPC, for all partition parameters p and all horizon lengths N. Indeed, S grows quadratically in the horizon N since the number of decision variables describing the PWA policies grows quadratically N. On the other hand, S-B is independent of the complexity of the PWA policies and solely depends on the dimension of the (original) uncertainty $\mathbf{w}$, and therefore grows linearly in N. Of course, the difference between S and S-B is more pronounced as the horizon becomes larger, and in the flexibility of the PWA policies p is increased. For example, for $N = 60$ and $p = 8$, S is two orders of magnitude larger than S-B. From a pure sampling-based point of view, we conclude that RMPC-B requires much fewer samples, which can be advantageous in cases in which the generation of samples itself is computationally demanding. Nevertheless, the smaller sample size does not automatically imply less conservative solutions, as the constraints need to satisfied for all uncertainty realizations inside the generated set $\mathbb{B} \cap \mathbb{W}$. Indeed, as reported in [60, Section V-B], for problem instances of RMPC-B(1), the "box-approach" can become substantially more conservative than RMPC(1) despite a smaller sample size. We will return to this in the Subsection 3.5.3.

Table 5: *Comparison of the sample sizes for for RMPC(p) and RMPC-B(p) with $\epsilon = 0.1$, $\beta = 10^{-7}$.*

Horizon	$p = 1$		$p = 4$		$p = 8$	
	RMPC	RMPC-B	RMPC	RMPC-B	RMPC	RMPC-B
$N = 10$	1001	477	2664	477	4733	477
$N = 20$	2899	770	9261	770	17'419	770
$N = 30$	5797	1041	19'858	1041	38'105	1041
$N = 40$	9696	1301	34'456	1301	66'792	1301
$N = 50$	14594	1553	53'053	1553	103'478	1553
$N = 60$	20493	1801	75'651	1801	148'165	1801

3.5.2 Computational Complexity

In this section, we compare the computation complexity for solving RMPC(p) and RMPC-B(p) for $\epsilon = 0.1$ and $\beta = 10^{-7}$. All numerical experiments were carried out using the CPLEX [26] optimization package interfaced in Matlab via Yalmip [30], on a 64-bit Linux operating system, equipped with 128 GB RAM and a 16-core hyperthreaded Intel Xeon 2.6 GHz processor. Table 6 reports the (average) optimization time, and Table 7 reports the required memory allocation for RMPC(p).

Table 6 clearly shows computational benefits of RMPC-B(p) compared to RMPC(p). In particular, for fixed p, the solution time of RMPC-B(p) is at least one order of magnitude smaller than RMPC(p), with the relative gap in solution time increasing with the horizon N. This is not surprising since the number of constraints in RMPC(p) grows cubically in the horizon N, while the number of constraints in RMPC-B(p) grows only quadratically in N, see also Table 4. This result is also evident in Table 7, where the memory required by RMPC(p) is prohibitive for problem instances with $(N > 50, p \geq 1)$, $(N > 30, p \geq 4)$ and $(N > 20, p \geq 8)$. Note that the memory required by RMPC-B(p) is less than 5MB for all problem instances $N \leq 60$ and $p \leq 8$.

3.5.3 Objective value and empirical violation probability

In this section, we examine the objective values and a posteriori empirical violation probability of the solutions obtained by using RMPC(p) and RMPC-B(p), as a function of the

Table 6: *Comparison of solution time for RMPC(p) and RMPC-B(p) with $\epsilon = 0.1$, $\beta = 10^{-7}$.*

Horizon	$p = 1$ RMPC	$p = 1$ RMPC-B	$p = 4$ RMPC	$p = 4$ RMPC-B	$p = 8$ RMPC	$p = 8$ RMPC-B
$N = 10$	0.42 s	25 ms	3.9 s	78 ms	12.4 s	0.2 s
$N = 20$	12 s	0.2 s	3.6 min	0.6 s	11.9 min	1.5 s
$N = 30$	1.4 min	0.3 s	45 min	1.8 s	#	4.4 s
$N = 40$	7.8 min	1.0 s	#	3.6 s	#	12.0 s
$N = 50$	26.2 min	1.4 s	#	7.3 s	#	24.0 s
$N = 60$	#	2.2 s	#	11.9 s	#	46.2 s

#: Out of memory error from MATLAB.

Table 7: *Required memory allocation for RMPC(p) with $\epsilon = 0.1$, $\beta = 10^{-7}$.*

Horizon	$p = 1$ RMPC	$p = 4$ RMPC	$p = 8$ RMPC
$N = 10$	8.4 MB	77 MB	270 MB
$N = 20$	190 MB	2.2 GB	8.0 GB
$N = 30$	1.2 GB	16 GB	60 GB
$N = 40$	4.8 GB	65 GB	250 GB
$N = 50$	14 GB	200 GB	760 GB
$N = 60$	34 GB	480 GB	1.9 TB

complexity of the PWA policies p. For these computational experiments we fix $N = 10$, $\epsilon = 0.2$ and $\beta = 10^{-7}$. Our analysis is performed by means of Monte-Carlo simulations: For every multi-sample extraction of $\{\mathbf{w}^{(1)}, \mathbf{w}^{(2)}, \ldots\}$, we determined the objective value of the sampled program and its (empirical) constraint violation probability $\hat{\epsilon}$, which we estimate by evaluating the solution of the sampled problem against 10^4 new disturbance realizations. This process is repeated 10^3 times, through which we obtain the average cost and average constraint violation probability. Fig. 4 depicts the cost for both algorithms, with an increasing number of regions, while Fig. 5 shows the empirical violation probability.

In Fig. 4, we see that the cost for RMPC(p) and RMPC-B(p) decreases as a function of partitions p. This is intuitive since the increasing number of partitions induce greater flexibility to the PWA-policies. Notice that the decrease is not necessarily monotonic in p since the partitioning break points (i.e., the b_i's in Fig. 3) were chosen to be placed

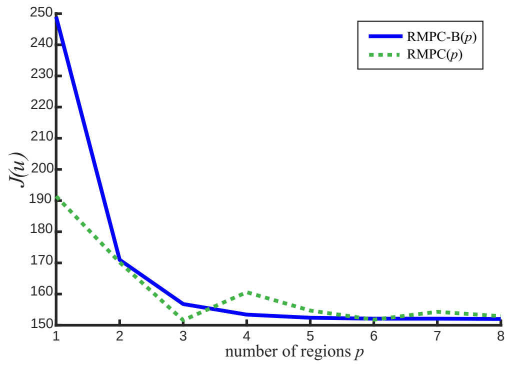

Figure 4: *Average cost of RMPC(p) and RMPC-B(p) for varying number of regions.*

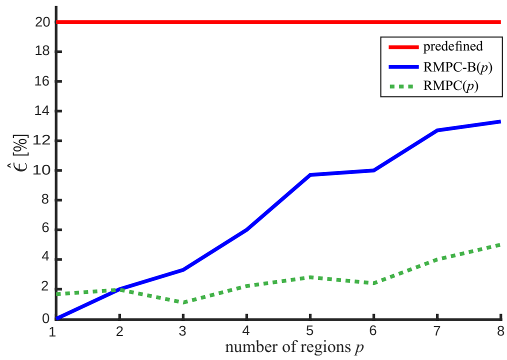

Figure 5: *Predefined ϵ ("red"), empirical estimate of ϵ for RMPC-B(p) ("blue") and empirical estimate of ϵ for RMPC(p) ("green").*

uniformly inside the uncertainty set $\mathbb{W}$. It is interesting to see that for small values of p, RMPC-B(p) is more conservative compared to RMPC(p), which verifies the observation made in [60, Section V-B]. This is the case since the box uncertainty constructed in (18) can include a much larger section of the original uncertainty set, compared to the convex hull of the underlying samples used. Nevertheless, with increased flexibility, problems RMPC(p) and RMPC-B(p) converge to the same cost, with RMPC-B(p) requiring only a fraction of computation time compared to RMPC(p).

With increased flexibility, a higher empirical violation probability is also achieved. This result is depicted in Fig. 5. The result is intuitive since PWA policies will naturally try to exploit the increased flexibility to reduce cost, at the expense of higher violation probabilities. Note, however, that the violation probabilities do not exceed the predefined level of $\epsilon = 0.2$, and therefore still remain conservative, especially for RMPC(p). This can be intuitively explained by the fact that while a large p provides more flexibility, more samples need to be extracted in RMPC(p) (c.f. Table 5). In contrast, the number of samples required by RMPC-B(p) remains the same independent of p, which leads to more conservative solutions in affine decision rules ($p = 1$), but improves as the number of partitions increases.

3.5.4 Conclusion

PWA policies applied to Randomized MPC problems generally produce less conservative results than the corresponding affine policies. Unfortunately, the straight forward application of Randomized MPC with PWA policies requires the solution of an optimization problem whose number of constraints scales cubicly in the prediction horizon, and can only be solved for small problem instances. We address this issue by proposing an alternative method based on a combination of randomized and robust optimization techniques. The size of the resulting optimization problem grows only quadratically in the prediction horizon. Numerical simulations show that the proposed approach is solved orders of magnitude faster than existing methods, while greatly reducing the conservatism compared to standard Randomized MPC apporaches using affine policies. Future work concentrate on incorporating a constraint removal scheme to further improve objective value.

4 Summary

In this deliverable, we address the following: (*i*) we utilize solution techniques partly developed and presented in Deliverable 3.3 to formulate and solve a building control problem, which is one of the case studies of L4G. Our results demonstrate that the proposed solution technique can provide high quality control designs to a computationally intractable optimization problem such as the building control problem, that outperform the state of the art solution techniques for stochastic control problems; and (*ii*) We proposed a novel approximation for addressing chance-constrainted, multistage optimization problems. This type of problem structure are very common in Stochastic Model Predictive Control problems for constrained linear systems subject to additive disturbance. The approximation is presented from a centralized optimization point of view, but our results can readily be extend to distributed problems using the solution method proposed and presented in Section 5 of Deliverable 3.3, which is based on the alternating direction method of multipliers. In collaboration with the project partners from RWTH Aachen University, we are currently testing the performance of the proposed methods in a simulated environment, prior to the actual implementation on the real system.

The next deliverable, Deliverable 4.1.2, will extend the methodology to cover non-linear dynamical systems that can be controlled using decentralised optimization schemes. To this end, we are currently working towards two solution methods based on approximated dynamic programming. The first method tries to exploit sparsity structures for the so called *Q-function* (defined in Section 3.4.2 of Deliverable 3.3). Given the centralised optimization problem, the proposed methodology allows to construct a finite number of decoupled optimization problems that can be solved independently leading to a decentralised solution scheme for the centralised optimization problem. The second method combines ideas from approximate dynamic programming and decision rules and create a novel approach for the construction of feedback policies with a pre-specified distributed structure. The methodology promises to deliver a fast computational solution method for a class of problems that are considered computational intractable.

References

[1] M. Arnold, R.R. Negenborn, G. Andersson, and B. De Schutter. Distributed predictive control for energy hub coordination in coupled electricity and gas networks. In *Intelligent Infrastructures*, pages 235–273. Springer, 2010.

[2] A. Aswani, N. Master, J. Taneja, D. Culler, and C. Tomlin. Reducing transient and steady state electricity consumption in hvac using learning-based model-predictive control. *Proceedings of the IEEE*, 100(1):240–253, 2012.

[3] A. Ben-Tal, L. El Ghaoui, and A. Nemirovski. *Robust Optimization*. Princeton University Press, 2009.

[4] A. Ben-Tal, A. Goryashko, E. Guslitzer, and A. Nemirovski. Adjustable robust solutions of uncertain linear programs. *Mathematical Programming*, 99(2):351–376, 2004.

[5] S. Bengea, A. Kelman, F. Borrelli, R. Taylor, and S. Narayanan. Implementation of model predictive control for an hvac system in a mid-size commercial building. *HVAC&R Research*, 20(1):121–135, 2014.

[6] G. Calafiore and L. Fagiano. Stochastic Model Predictive Control of LPV Systems via Scenario Optimization. *Automatica*, 49(6):1861–1866, 2013.

[7] Giuseppe Carlo Calafiore. Random convex programs. *SIAM Journal of Optimization*, 20(6):3427–3464, 2010.

[8] Giuseppe Carlo Calafiore and Marco Claudio Campi. Uncertain convex programs: Randomized solutions and confidence levels. *Mathematical Programming, Series A*, 102:25–46, 2005.

[9] Giuseppe Carlo Calafiore and Marco Claudio Campi. The scenario approach to robust control design. *IEEE Transactions on Automatic Control*, 51(5):742–753, 2006.

[10] Marco Claudio Campi and Simone Garatti. The exact feasibility of randomized solutions of uncertain convex programs. *SIAM Journal of Optimization*, 19:1211–1230, 2008.

[11] M. Cannon, B. Kouvaritakis, and Xingjian Wu. Probabilistic Constrained MPC for Multiplicative and Additive Stochastic Uncertainty. *IEEE Transactions on Automatic Control*, 54(7):1626–1632, 2009.

[12] Mark Cannon, Basil Kouvaritakis, Saša V Raković, and Qifeng Cheng. Stochastic tubes in model predictive control with probabilistic constraints. *Automatic Control, IEEE Transactions on*, 56(1):194–200, 2011.

[13] Mark Cannon, Basil Kouvaritakis, and Xingjian Wu. Model predictive control for systems with stochastic multiplicative uncertainty and probabilistic constraints. *Automatica*, 45(1):167–172, 2009.

[14] D. Crawley, L. Lawrie, C. Pedersen, and F. Winkelmann. Energy plus: energy simulation program. *ASHRAE journal*, 42(4):49–56, 2000.

[15] EN 15251:2007. Indoor environmental input parameters for design and assessment of energy performance of buildings addressing indoor air quality, thermal environment, lighting and acoustics. european committee for standardization, 2007.

[16] R. Evins, K. Orehounig, V. Dorer, and J. Carmeliet. New formulations of the energy hub model to address operational constraints. *Energy*, 73:387–398, 2014.

[17] E. Fabrizio, M. Filippi, and J. Virgone. An hourly modelling framework for the assessment of energy sources exploitation and energy converters selection and sizing in buildings. *Energy and Buildings*, 41(10):1037–1050, 2009.

[18] H. Fakham, P. Degobert, and B. François. Control system and power management for a PV based generation unit including batteries. In *International Aegean Conference on Electrical machines and power electronics, ACEMP'07.*, pages 141–146. IEEE, 2007.

[19] M. Geidl and G. Andersson. Optimal coupling of energy infrastructures. In *Power Tech, 2007 IEEE Lausanne*, pages 1398–1403. IEEE, 2007.

[20] M. Geidl, G. Koeppel, P. Favre-Perrod, B. Klockl, G. Andersson, and K. Frohlich. Energy hubs for the future. *IEEE Power and Energy Magazine*, 5(1):24–30, 2007.

[21] Abebe Geletu, Michael Klöppel, Armin Hoffmann, and Pu Li. A tractable approximation of non-convex chance constrained optimization with non-gaussian uncertainties. *Engineering Optimization*, 47(4):495–520, 2015.

[22] Abebe Geletu, Michael Klöppel, Hui Zhang, and Pu Li. Advances and applications of chance-constrained approaches to systems optimisation under uncertainty. *International Journal of Systems Science*, 44(7):1209–1232, 2013.

[23] A. Georghiou, W. Wiesemann, and D. Kuhn. Generalized decision rule approximations for stochastic programming via liftings. *Mathematical Programming*, pages 1–38, 2014.

[24] Angelos Georghiou, Wolfram Wiesemann, and Daniel Kuhn. Generalized decision rule approximations for stochastic programming via liftings. *Mathematical Programming*, pages 1–38, 2014.

[25] P.J. Goulart, E.C. Kerrigan, and J.M. Maciejowski. Optimization over state feedback policies for robust control with constraints. *Automatica*, 42:522–533, 2006.

[26] IBM ILOG. CPLEX Optimization Studio. [online] `http://www-01.ibm.com/software/integration/optimization/cplex-optimization-studio/`. last accessed March 09, 2013.

[27] Mayuresh V. Kothare, Venkataramanan Balakrishnan, and Manfred Morari. Robust constrained model predictive control using linear matrix inequalities. *Automatica*, 32(10):1361 – 1379, 1996.

[28] D. Kuhn, W. Wiesemann, and A. Georghiou. Primal and dual linear decision rules in stochastic and robust optimization. *Mathematical Programming*, 130(1):177–209, 2011.

[29] J. Laustsen. Energy efficiency requirements in building codes, energy efficiency policies for new buildings. *International Energy Agency (IEA)*, pages 477–488, 2008.

[30] J. Löfberg. YALMIP: A toolbox for modeling and optimization in MATLAB. *IEEE International Symposium on Computer Aided Control Systems Design*, pages 284–289, 2005.

[31] Johan Löfberg. *Minimax approaches to robust model predictive control.* PhD thesis, Linksping University, 2003.

[32] James Luedtke and Shabbir Ahmed. A sample approximation approach for optimization with probabilistic constraints. *SIAM Journal on Optimization*, 19(2):674–699, 2008.

[33] M. Maasoumy, M. Razmara, M. Shahbakhti, and A. Vincentelli. Handling model uncertainty in model predictive control for energy efficient buildings. *Energy and Buildings*, 77:377–392, 2014.

[34] K. Margellos, P. Goulart, and J. Lygeros. On the road between robust optimization and the scenario approach for chance constrained optimization problems. *IEEE Transactions on Automatic Control*, 59(8):2258–2263, 2014.

[35] D.Q. Mayne, M.M. Seron, and S.V. Raković. Robust model predictive control of constrained linear systems with bounded disturbances. *Automatica*, 41:219–224, 2005.

[36] J. McQuade. A system approach to high performance buildings. Technical report, United Technologies Corporation, 2009.

[37] A Nemirovski and A. Shapiro. Scenario approximations of chance constraints. In *Probabilistic and randomized methods for design under uncertainty*, pages 3–48. Springer, 2006.

[38] F. Oldewurtel, A. Parisio, C. N. Jones, D. Gyalistras, M. Gwerder, V. Stauch, B. Lehmann, and M. Morari. Use of model predictive control and weather forecasts for energy efficient building climate control. *Energy and Buildings*, 45:15–27, 2012.

[39] Frauke Oldewurtel, Colin N Jones, and Manfred Morari. A tractable approximation of chance constrained stochastic MPC based on affine disturbance feedback. In *Proc. of the IEEE Conf. on Decision and Control*, pages 4731–4736, 2008.

[40] BK Pagnoncelli, Shapiro Ahmed, and A Shapiro. Sample average approximation method for chance constrained programming: theory and applications. *Journal of optimization theory and applications*, 142(2):399–416, 2009.

[41] A. Parisio, C. Del Vecchio, and A. Vaccaro. A robust optimization approach to energy hub management. *International Journal of Electrical Power & Energy Systems*, 42(1):98–104, 2012.

[42] Alessandra Parisio, Damiano Varagnolo, Marco Molinari, Giorgio Pattarello, Luca Fabietti, and Karl H Johansson. Implementation of a scenario-based MPC for HVAC systems: an experimental case study. *Preprints of the 19th World Congress, The International Federation of Automatic Control. School of Electrical Engineering, Royal Institute of Technology, Osquldas vg*, 10:10, 2014.

[43] Maria Prandini, Simone Garatti, and John Lygeros. A randomized approach to stochastic model predictive control. In *Proc. of the IEEE Conf. on Decision and Control*, 2012.

[44] Georg Schildbach, Lorenzo Fagiano, Christoph Frei, and Manfred Morari. The scenario approach for stochastic model predictive control with bounds on closed-loop constraint violations. *Automatica*, 50(12):3009 – 3018, 2014.

[45] Georg Schildbach, Lorenzo Fagiano, and Manfred Morari. Randomized solutions to convex programs with multiple chance constraints. *SIAM Journal on Optimization*, 23(4):2479–2501, 2013.

[46] P.O.M. Scokaert and D.Q. Mayne. Min-max feedback model predictive control for constrained linear systems. *IEEE Transactions on Automatic Control*, 43(8):1136 – 1142, 1998.

[47] J. Siroky, F. Oldewurtel, J. Cigler, and S. Privara. Experimental analysis of model predictive control for an energy efficient building heating system. *Applied Energy*, 88(9):3079–3087, 2011.

[48] D. Sturzenegger. *Model Predictive Building Climate Control - Steps Towards Practice*. PhD thesis, ETH Zurich, Zürich, December 2014.

[49] D. Sturzenegger, D. Gyalistras, M. Gwerder, C. Sagerschnig, M. Morari, and R. S. Smith. Model predictive control of a swiss office building. In *11th REHVA World Congress Clima*, 2013.

[50] D. Sturzenegger, D. Gyalistras, V. Semeraro, M. Morari, and R. S. Smith. BRCM Matlab Toolbox: Model generation for model predictive building control. In *American Control Conference*, pages 1063–1069, Portland, June 2014.

[51] Roberto Tempo, Giuseppe Calafiore, and Fabrizio Dabbene. *Randomized algorithms for analysis and control of uncertain systems: with applications*. Springer Science & Business Media, 2012.

[52] Vladimir Naumovich Vapnik and Vlamimir Vapnik. *Statistical learning theory*, volume 1. Wiley New York, 1998.

[53] Phebe Vayanos, Daniel Kuhn, and Berc Rustem. A constraint sampling approach for multi-stage robust optimization. *Automatica*, 48(3):459 – 471, 2012.

[54] M. Vidyasagar. Statistical learning theory and randomized algorithms for control. *Control Systems, IEEE*, 18(6):69–85, Dec 1998.

[55] M Vidyasagar. Randomized algorithms for robust controller synthesis using statistical learning theory. *Automatica*, 37(10):1515–1528, 2001.

[56] E. I. Vrettos and S. A. Papathanassiou. Operating policy and optimal sizing of a high penetration res-bess system for small isolated grids. *IEEE Transactions on Energy Conversion*, 26(3):744–756, 2011.

[57] X. Zhang, S. Grammatico, G. Schildbach, P. Goulart, and J. Lygeros. On the sample size of randomized mpc for chance-constrained systems with application to building climate control. In *European Control Conference (ECC)*, pages 478–483, 2014.

[58] X. Zhang, S. Grammatico, G. Schildbach, P. Goulart, and J. Lygeros. On the sample size of randomized MPC for chance-constrained systems with application to building climate control. In *European Control Conference*, Strasbourg, France, 2014.

[59] X. Zhang, S. Grammatico, Georg Schildbach, P.J. Goulart, and John Lygeros. On the sample size of random convex programs with structured dependence on the uncertainty. In *Automatica (accepted)*, 2015.

[60] X. Zhang, K. Margellos, P. Goulart, and J. Lygeros. Stochastic model predictive control using a combination of randomized and robust optimization. In *Proc. of the IEEE Conf. on Decision and Control*, Florence, Italy, 2013.

[61] X. Zhang, G. Schildbach, D. Sturzenegger, and M. Morari. Scenario-based mpc for energy-efficient building climate control under weather and occupancy uncertainty. In *European Control Conference (ECC)*, pages 1029–1034. IEEE, 2013.

[62] Xiaojing Zhang, Georg Schildbach, David Sturzenegger, and Manfred Morari. Scenario-Based MPC for Energy-Efficient Building Climate Control under Weather and Occupancy Uncertainty. In *Proc. of the European Control Conference*, pages 1029–1034, 2013.